

Summary for Policymakers

# Korean Climate Change Assessment Report 2020

- The Physical Science Basis -



ISBN 978-89-954715-9-3

# **Korean Climate Change Assessment Report 2020**

**- The Physical Science Basis -**

---

**Summary for Policymakers**

---



Korea Meteorological  
Administration



# Contents

---

<b>1. Introduction</b>	<b>1</b>
1.1. Background and procedure	1
1.2. A summary of 「Korean climate change assessment report 2014」	2
1.3. Main results of the National Institute of Meteorological Research 「global climate projection to IPCC 6th assessment report」	3

---

<b>2. Observation: Atmosphere and Land</b>	<b>5</b>
2.1. Introduction	5
2.2. Changes in atmospheric composition and radiation	5
2.3. Change in temperature	5
2.4. Water cycle change	6
2.5. Changes in extreme events	7
2.6. Changes in pattern of large-scale atmospheric circulation and its variability	7

---

<b>3. Observation: Ocean and Cryosphere</b>	<b>9</b>
3.1. Introduction	9
3.2. Ocean	9
3.3. Cryosphere	10

---

<b>4. Information from Palaeoclimate Archive</b>	<b>13</b>
4.1. Introduction	13
4.2. Pollen	13
4.3. Animal	13
4.4. Tree-ring	14
4.5. Old documents	16

---

<b>5. Carbon and Other Biogeochemical Cycle</b>	<b>17</b>
5.1. Introduction	17
5.2. Carbon cycle	17
5.3. Other biogeochemical cycle	19

# Contents

---

<b>6. Clouds and Aerosols</b>	<b>21</b>
6.1. Introduction	21
6.2. Clouds	21
6.3. Aerosols	21
6.4. Aerosol-cloud interaction	22
6.5. Radiative forcing and effective radiative forcing	24
6.6. Processes of precipitation change	24

---

<b>7. Anthropogenic and Natural Radiative Forcing</b>	<b>25</b>
7.1. Introduction	25
7.2. Tropospheric ozone	25
7.3. Anthropogenic radiative forcing	26
7.4. Natural effect of radiative forcing	27
7.5. Emission metrics	27

---

<b>8. The Evaluation of Climate Model</b>	<b>29</b>
8.1. Introduction	29
8.2. Global climate model	29
8.3. Regional climate model downscaling	30
8.4. Regional coupled model	31
8.5. Simulation of extreme events	32

---

<b>9. Detection of Climate Change and Changes in Meteorological Disasters on the Korean Peninsula</b>	<b>33</b>
9.1. Introduction	33
9.2. Temperature and precipitation changes in East Asia and the Korean Peninsula	33
9.3. Changes in climate variability and their impacts on the Korean Peninsula	34
9.4. Changes in meteorological disasters on the Korean Peninsula	36

---

<b>10. Short-term and Long-term Projections of Climate Change</b>	<b>37</b>
10.1. Introduction	37
10.2. Atmosphere and indicators	37
10.3. The ocean and the cryosphere	39
10.4. 1.5°C Climate change projection	40



# 1. Introduction



## 1.1. Background and procedure

Every five or six years, the IPCC (Intergovernmental Panel on Climate Change) publishes a report aimed at aiding climate change adaption and damage reduction. This report includes the latest studies on global climate change.

To support the establishment of national policies for climate change adaptation, the Korean government has published a climate change assessment report every five years since 2011. This report includes the results of climate change studies on Korea, and is based on the IPCC assessment reports.

An assessment of climate change in Korea is needed to establish the third national climate change adaptation policy (21~25). The 「Korean climate change assessment report 2020」 should reflect and complement the recent researches that was based on the 「Korean climate change assessment report 2014」 published in 2014.

The publication of the 2020 report has led to national policies that support climate change adaptation. This report will also contribute to the IPCC's 6th assessment report, reflecting the recent results of climate change research in Korea.

To prepare the 「Korean climate change assessment report 2020」, the Korea Meteorological Administration (KMA) and the Ministry of Environment (ME) are responsible for the first (scientific basis) and the second (effects and adaptations) working group, respectively. The authors of the “scientific basis” group prepared the report according to the following guidelines.

- The chapter titles should be the same as in the 「Korean climate change assessment report 2014」,

with the exception of chapter 9.

- The main text of each chapter should be composed of research results by subject. Each chapter should begin with a summary of the 「Korean climate change assessment report 2014」 with new studies for 2014~2019 added.
- The level of agreement for the results given in each chapter should be evaluated in three stages (Table 1.1).
- The references are to be confined to papers or reports published since 2014; however, studies missing from the 「Korean climate change assessment report 2014」 can also be included.

**Table 1.1. Framework for assessing the reliability (agreement level) of the studies described in the report.**

<b>01</b> Solid agreement	The number of papers is sufficient and they are consistent with one another, or there is a general consensus among experts.
<b>02</b> Intermediate agreement	There is agreement among a certain number of papers, but it is difficult to make a judgment of the evidence due to the existence of minority opinions, or there are different opinions among experts.
<b>03</b> Limited agreement	The number of relevant papers is a small, or the opinions of experts are different, making it difficult to determine the reliability of a given conclusion.

The Korean climate change assessment report is mainly based on the IPCC report and is organized according to Korea's particular circumstances. 「Korean climate change assessment report 2020」 consists of ten

chapter: 'CH<sub>1</sub> Introduction', 'CH<sub>2</sub> observation: atmosphere and surface', 'CH<sub>3</sub> observation: ocean and cryosphere', 'CH<sub>4</sub> information from paleoclimate archive', 'CH<sub>5</sub> carbon cycle and other biogeochemical cycle', 'CH<sub>6</sub> clouds and aerosols', 'CH<sub>7</sub> anthropogenic and natural radiative forcing', 'CH<sub>8</sub> the evaluation of climate model', 'CH<sub>9</sub> detection of climate change and changes in meteorological disasters on the Korean Peninsula', and 'CH<sub>10</sub> short-term and long-term projections of climate change'.

The report has some limitations. Due to the lack of domestic research, the chapters related to observational studies evaluate the results based on limited data. For the future, continuous observational studies are required.

To aid in climate change studies and policy decisions, the level of agreement among research results is shown in the conclusion to each chapter (Table 1.1). This level is determined by the number of papers and expert opinion only. Given the importance of determining the level of agreement, objective standards are needed to decide on this level.

---

## 1.2. A summary of 'Korean climate change assessment report 2014'

The atmospheric concentrations of CO<sub>2</sub> (carbon dioxide) and N<sub>2</sub>O (nitrous oxide), two main greenhouse gases, clearly increased between 2004 and 2013. From 2001 to 2010 the annual mean precipitation over Korea was 7.4% higher than for the last 30 years, with the increase in summer being the most obvious. In the 1980s, there had been a weakening of the East Asian summer monsoon, but its intensity has increased again since the 2010s. The intensity of the Siberian High, which affects the winter monsoon, has shown evident decadal variability.

The sea surface temperature and sea level in the seas around Korea have been continuously rising at rates

about two to three times higher than the global mean. In the Arctic, there was a steep increase in temperatures of about 0.7°C for the 30 years up to 2013: this increase was largest in autumn. Warming trends have been observed in the west of the Antarctic Peninsula during August.

Pollen analysis shows that there have been changes in vegetation resulting from the changes in climate from the last Pleistocene glacial period to the present. The longest tree-ring chronology for Korea (1178-present), which is based on pine trees, was introduced in 2014 report, and the climate reconstructions based on the tree-ring data were summarized. Among the papers on temperature and precipitation that had been published by 2014, the longest reconstructions covered the periods from 1595 to the present and 1682 to the present, respectively.

As a component of the climate system, the carbon cycle is associated with complex forcing, nonlinear responses, and feedbacks at various scales due to climate change. In addition, the carbon cycle is connected to other biogeochemical cycles, which means that climate change can lead to serious impacts on the health of the ecosystem, as well as to pollution and effects on air quality.

Although some observational studies on the optical and physical properties of aerosols have been carried out, the number of cloud studies has been insufficient. The direct and indirect effects of aerosols and also cloud-precipitation interactions have been studied based on numerical models, but this has not been a very active area of research.

It has been reported that 30% of the increase in ozone concentration in East Asia in spring can be explained by the variability of certain meteorological factors. The amount of radiative forcing due to soot in East Asia has been estimated at +2.1 Wm<sup>-2</sup>, which is higher than the global radiative forcing due to CO<sub>2</sub> (+1.82 Wm<sup>-2</sup>). The global warming potential (GWP) has been used for assessing the environmental impact of

greenhouse gases since 2010.

Report 2014 mainly covered the evaluations of models which participated in the IPCC's 5<sup>th</sup> assessment report. With the model improvement from CMIP3 (Coupled Model Intercomparison Project Phase 3) to CMIP5 group for scenario projections, the atmosphere and ocean models had been simulated in higher resolution and improved to the direction to include aerosol process and carbon cycle. Overall, the simulation of the surface temperature was improved, but the precipitation simulation showed no significant improvement. For regional model, results from the COordinated Regional climate Downscaling Experiment (CORDEX) project were mainly reported and based on the CMIP3.

The 2014 report was mainly concerned with the evaluation of models that had featured in the IPCC's 5th assessment report. With the model improvement from CMIP3 (Coupled Model Intercomparison Project Phase 3) to CMIP5 group for scenario projections, the atmosphere and ocean models had been simulated in higher resolution and improved to the direction to include aerosol process and carbon cycle. Overall, the simulation of surface temperature has been improved, but there has been no significant improvement in the precipitation simulations. For the regional modeling, the main results were taken from the COordinated Regional climate Downscaling Experiment (CORDEX) and were based on CMIP3.

The annual mean temperature in Korea has increased significantly since the 1980s. Annual precipitation has also increased, mainly due to the increase in summer. The maximum amount of rainfall during Changma now occurs about a week earlier than in previous years. It has been suggested that the intensity of typhoons affecting the Korean Peninsula has increased. In addition, two types of El-Niño induce different seasonal teleconnections, which affect the climate of the Korean Peninsula. During negative phases of the Arctic Oscillation, East Asia experiences an enhanced

winter monsoon and frequent cold surges. In addition, since the late 1970s, both the intensity and frequency of tropical intra-seasonal oscillations have increased.

According to RCP4.5 (Representative Concentration Pathway 4.5) and RCP8.5, respectively. The annual mean temperature on the Korean Peninsula is projected to increase by 2°C or 4°C by the late 21<sup>st</sup> century. The precipitation increase in summer is projected to be greater than in winter; however, there is a high degree of uncertainty in these projections, which are also highly region-dependent. It is predicted that the number of days with heavy rainfall, heatwave days, tropical nights, and cooling degree days will increase, whereas the number of frost days, freezing days, and heating degree days will decrease

---

### 1.3 Main results of the National Institute of Meteorological Research 「global climate projection to IPCC 6th assessment report」

The Working Group on Coupled Models (WGCM) under the World Climate Research Program (WCRP), co-organized by the IPCC and the World Meteorological Organization (WMO), has driven CMIP6 since 2014. The main discussion in CMIP6 concerns sources of climate forcing, including new future paths for greenhouse gas concentrations, the design of scientific experiments, and the standardization of post-processing for model data. The National Institute of Meteorological Research (NIMR) has also followed this standardization in producing its climate change scenarios.

Climate forcing is used in standard, historical, and scenario experiments for evaluating the performance of models, simulating past climates, and making projections for the future. The climate forcing used in experiments consists of both anthropogenic and natural forcing.

The IPCC's 6<sup>th</sup> assessment report includes a new scenario called Shared Socio-economic Pathways (SSP). This consists of a set of social and economic structural changes and greenhouse gas reduction policies. In particular, the CMIP6 first establishes four standard SSP scenarios in conjunction with the RCP used in the 5th assessment report. The NIMR analyzed future global prospects based on the SSP1-2.6 and SSP5-8.5 scenarios of low and high emissions of greenhouse gases, respectively, and, based on this, published the 「Global climate change prospect report to IPCC AR6」.

The new forecast based on SSP shows that global mean temperature at the end of the 21<sup>st</sup> century will be approximately 1.9°C - 5.2°C higher than at present. This exceeds the temperature change of 1.3°C - 3.7°C in RCP 2.6 and RCP 8.5 produced by HadGEM2-AO.

In the same scenario, the global mean precipitation increases by about 5% - 10% compared with the present. In particular, the increase in precipitation is greatest in the polar regions with the greatest temperature increase and in equatorial regions with the most precipitation.

According to SSP5-8.5, the global mean sea surface temperature and sea level are expected to increase by about 1.4°C - 3.7°C and 52 cm - 91 cm, respectively, relative to the present by the end of the 21<sup>st</sup> century. In particular, it is predicted that the Arctic sea ice will almost disappear after the middle of the century and that the Antarctic sea ice will disappear by the end of the century.

In terms of extreme events, the number of extremely warm days will increase by about 15 days per decade, whereas the number of extremely cold days will decrease by about 4 days per decade. Although the change in the number of days with precipitation by the end of the 21<sup>st</sup> century is not clear, the frequency and intensity of extreme precipitation are predicted to increase relative to the present. In particular, in SSP5-8.5, the maximum five-day precipitation is expected to increase by approximately 29%, and the number of

days with extreme precipitation exceeding the 95th percentile is expected to increase by about 1.5 times.

## 2. Observation: Atmosphere and Surface



### 2.1. Introduction

The variability in the temperature and precipitation in Korea is directly influenced by the warming trend experienced by the globe in the recent past. This chapter describes the atmospheric and land-surface changes that have occurred in Korea, including changes in atmospheric composition, radiation, temperature, land cover, the water cycle, extreme events, atmospheric circulation, and climate variability, since the mid-2000s.

### 2.2. Changes in atmospheric composition and radiation

The concentrations of greenhouse gases including carbon dioxide (CO<sub>2</sub>) and methane (CH<sub>4</sub>) have been increasing in the Korean Peninsula during the past ten years (2008~2018) (solid agreement). In addition, the concentrations of other gases (ozone (O<sub>3</sub>), carbon monoxide (CO), nitrogen dioxide (NO<sub>2</sub>), and sulfur dioxide (SO<sub>2</sub>)) show various.

The CO<sub>2</sub> concentration measured at Anmyeondo was 415.2 ppm in 2018. Compared with the annual mean concentration of 371.2 ppm in 1999, this is an increase of 44 ppm in 19 years. The CO<sub>2</sub> concentration observed at Anmyeondo has increased at a rate of 2.4 ppm/year over the past ten years, which is similar to the mean global rate of 2.2 ppm/year (Figure 2.1).

The concentration of sulfur hexafluoride (SF<sub>6</sub>) is steadily increasing, but the concentration of CFCs has

been decreasing in recent years. Changes in the concentrations of other major greenhouse gases (O<sub>3</sub>, CO, NO<sub>2</sub>, and SO<sub>2</sub>) show different increasing trends. Since the 1990s, the O<sub>3</sub> concentration has increased steadily, whereas CO and SO<sub>2</sub> concentrations have decreased. The change in NO<sub>2</sub> concentration is not clear. The amounts of downward solar radiation and net radiation have not significantly changed and have shown only weak variability in the recent past.

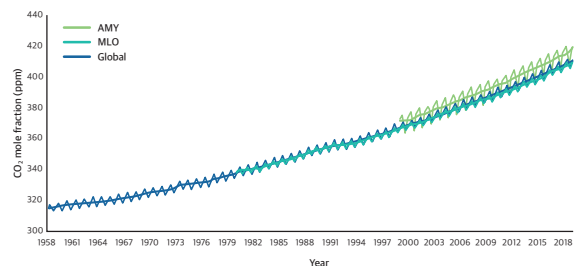


Fig. 2.1. Changes in CO<sub>2</sub> concentration at Anmyeondo (black, AMY), Mauna Loa (blue, MLO), and global (red, Global) (KMA (2019))

### 2.3. Change in temperature

Considering that the annual mean surface air temperature (SAT) recorded 13.0°C in the 2000s (2011~2017), the warming of South Korea is still continuing (12.2°C, 12.6°C, and 12.8°C in the 1980s, 1990s, and 2000s, respectively) (solid agreement). The warming trend was clear in almost regions, however, its magnitude was region-dependent in South Korea. Large cities

tend to have a strong warming tendency due to their urbanization effect (limited agreement).

After the annual mean SAT in South Korea recorded 13.6°C in 1998 (the second highest year since 1973), the overall warming trend has been slightly weakened (Figure 2.2). This may indicate that the influence of global warming hiatus during 1998~2013 also appears in South Korea based on the SAT averaged in 6 stations and 45 stations, respectively. However, the occurrences of warm years of 2015 (the top 3) and 2016 (the top 1) indicate that the warming is still continuing.

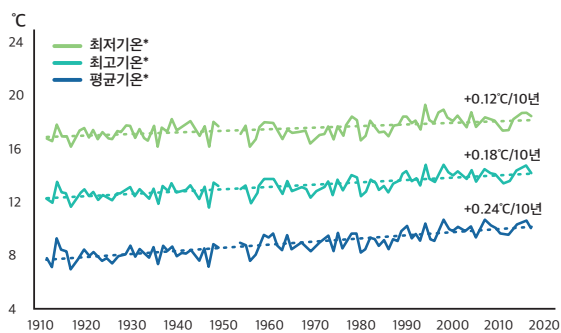


**Fig. 2.2. Time series of annual maximum, mean, and minimum temperature in South Korea for 1912~2017 (NIMR, 2018).**

After the annual mean temperature recorded in South Korea reached 13.6°C in 1998 (the second highest annual figure since 1973), the overall warming trend slightly weakened (Figure 2.2). Based on the SAT averages for 6 sites and 45 stations, respectively, this may indicate that the global warming hiatus of 1998~2013 also influenced South Korea. However, the occurrence of warm years in 2015 (third warmest) and 2016 (warmest) indicates that the warming is continuing.

Although the spatial distribution of warming in South Korea reveals some differences in intensity between observation stations, the warming trend (-0.04~0.61°C/10 years) since 1973 is apparent at all stations except Mungyeong and Gyeongbuk. Although there are no clear systematic differences in the warming

between, for example, the north and south, east and west, or coastal and inland areas, the warming trend has tended to be stronger in big cities that have experienced rapid urbanization and population growth since 1973.

The decrease in soil moisture in east Asia, including the Korean Peninsula, in summer is noticeable. As a result of comparing the soil moisture trends observed in satellite, ground observation, and reanalysis data from the summer seasons for the period 1996~2010, the decreasing trend in soil moisture in northern China region was found to be statistically significant. A decreasing trend was also found for the Korean Peninsula, but it was not statistically significant.

## 2.4. Water cycle change

The linear trend in precipitation over the Korean peninsula is strongest during boreal summer (June–July–August) as +11.6 mm/10year during 1912~2017, and those during the other seasons (i.e., boreal spring, fall, and winter) is unclear (intermediate agreement).

The linear trend in precipitation over the Korean peninsula is strongest during the boreal summer. The linear trend in the summer precipitation is +11.6 mm/10 years for the period 1912~2017. The corresponding observed trends for the boreal fall and spring seasons are +3.9 mm/10 years and +1.9 mm/10 years, respectively, and thus these trends are systematically weaker than those for the boreal summer season. The linear trend in precipitation during the boreal winter season is -0.9 mm/10 years, which means that no increasing trend is observed. As well as the climatological precipitation, the intensity, the inter-annual variation in, and the driving mechanism of the summer precipitation can change due to global warming; however, it is still

unclear whether the inter-annual variation in precipitation has significantly changed due to global warming.

The linear trend in the water vapor flux cannot be clearly observed, which is consistent with the insignificant increasing trend in wave vapor flux over the north Pacific between 1983 and 2017. Also, the amount of evapotranspiration in the major cities in Korea shows diverse linear trends; therefore, it is premature to draw conclusions concerning the impact of global warming on evapotranspiration over the Korean Peninsula.

## 2.5. Changes in extreme events

Probability and intensity of heat wave in spring show the pronounced increase over South Korea after mid-2010s, particularly in May (solid agreement). Frequency of warm extremes in summer has been rapidly increasing since mid-1990s, exhibiting a marked shift particularly after mid-2010s (intermediate agreement). Winter cold extremes tend to be intensified after 2000s (limited agreement).

The increasing yearly temperature trend in Korea before 2000 was mainly driven by strong seasonal warming in winter. After 2000, however, there was a cooling trend in winter, whereas the warming trend in summer became stronger (Table 2.1).

**Table 2.1. Trends in seasonal mean temperature during the period 1960~2012 based on 11 observation stations in Korea (°C/10 years) (Min et al., 2015). \* indicates significant trend at 95% confidence level.**

	1960~2012	1960~1999	2000~2012
Annual T <sub>mean</sub>	0.23	0.27	0.17
Winter T <sub>mean</sub>	0.32	0.50*	-0.85
Summer T <sub>mean</sub>	0.09	0.03	0.65

The increasing probability of warm extremes in monthly average temperatures over the past 10 years is pronounced, particularly for May. The warmest average temperature for May was recorded in 2012, which was followed by consecutive years of record-breaking May temperatures during 2014~2017. May 2019 was ranked as the second warmest, and the top five warmest Mays all occurred after 2014. Consistent with this, a distinct summer warming trend can be observed beginning in the mid-1990s, accompanied by frequent occurrences of heatwaves over east Asia.

There has been a change in the winter temperature trend from negative to positive, which is related to the intensification of cold waves since 2000. Changes in the characteristics of cold waves that occurred in the 1980s and 2000s can be widely observed across east Asia. The change that occurred in the 2000s can be attributed to a shift to the negative phase of the Arctic Oscillation, weakening of the stratospheric polar vortex, and the frequent development of Ural blocking. Summer precipitation shows a distinct increase since the mid-1990s, which is also consistent with observations for other regions of east Asia. However, beginning in the mid-2010s, the features of the precipitation anomalies are distinct from those of earlier periods. This requires further investigation.

## 2.6. Changes in pattern of large-scale atmospheric circulation and its variability

The East Asian winter monsoon strengthened during the 10 years since 2000. This was mainly associated with factors including changes in the intensity of the Siberian High, Eurasian snow cover, and the Arctic climate (intermediate agreement). Since the late 2000s, the frequency of El-Niño events has increased (intermediate agreement). The effect of the warming of the

Indian Ocean on the Korean climate is increasing, whereas the Atlantic Meridional Overturning Circulation is weakening (solid agreement).

East Asian winter monsoon has been strengthened for recent decades since the early 2000s as evidenced by frequent occurrence of extremely cold winters all over East Asia. This is in contrast to previous observations of weakening East Asian winter monsoon since the late 1980s. The strong winter monsoon in the 2000s, characterized by a negative temperature anomaly near the surface of Siberia, exhibits limited occupancy in the northern East Asia. The atmospheric circulation associated with the winter monsoon can be attributed to the teleconnections coming across the Eurasia.

Recent studies report weakening of the Atlantic Meridional Overturning Circulation. In line with this trend, the sea surface temperature of the North Atlantic Ocean in particular near the Greenland has shown a cooling trend. Declining trend in the Arctic sea ice extent has continued in the recent observation. For June, the trend is approximately 4.1% decline per decade (Fig. 2.3). The Antarctic sea ice extent, which is unlikely to make strong influence on East Asian climate, steadily increased until 2014, but from 2015, a steep declining has been observed.

The East Asian winter monsoon has strengthened since the early 2000s, as evidenced by the frequent occurrence of extremely cold winters across east Asia. This is in contrast to earlier observations of a weakening of the East Asian winter monsoon since the late 1980s. The strong winter monsoon in the 2000s, characterized by a negative temperature anomaly near the surface over Siberia, confines to the northern East Asia. The atmospheric circulation associated with the winter monsoon can be attributed to teleconnections coming across the Eurasia.

Recent studies have also reported a weakening of the Atlantic Meridional Overturning Circulation. As a result of this trend, the sea surface temperature of the North Atlantic Ocean near Greenland, in particular, has shown a cooling trend. The decline in Arctic sea ice extent has

continued recently. For June, the trend is a decline of approximately 4.1% per decade (Fig. 2.3). Antarctic sea ice extent, which is unlikely to have a strong influence on the east Asian climate, steadily increased up to 2014; however, since 2015, a steep decline has been observed.

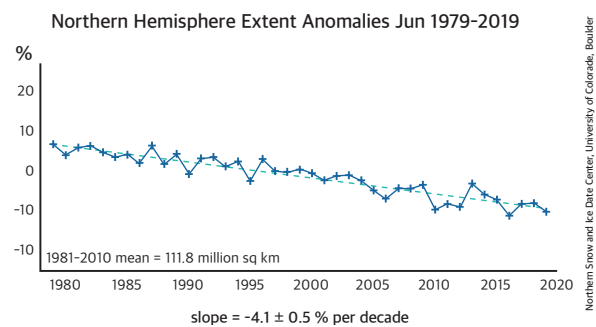


**Fig. 2.3. The trend of Arctic sea ice extent in June (NOAA NSIDC; [https://nsidc.org/data/seaice\\_index/compare\\_trends](https://nsidc.org/data/seaice_index/compare_trends))**

# 3. Observation: Ocean and Cryosphere



## 3.1. Introduction

The IPCC's "Special Report on the Ocean and Cryosphere (2019)" emphasized the importance of ocean and cryosphere responses. It was reported that the reductions in sea ice in the polar seas and in the volume of glaciers were continuing and that the amount of sea level rise was expected to be higher than the existing forecasts in climate change assessment reports. It was also suggested that the incidence of ocean-induced extreme phenomena would increase along with the continuing increase in ocean heat content. The cryosphere consists of snow and ice, which are sensitive to climate change and so respond more to the increase in greenhouse gases than to other components of the climate system. This chapter is concerned with observations of the ocean and cryosphere.

## 3.2. Ocean

The sea surface temperature and sea level in the seas around Korea have been rising at a higher rate than the global average, and ocean acidification has been continuing (solid agreement). In addition, in recent years, the frequency of ocean extremes, such as polarization of the water temperature, has increased (intermediate agreement).

It has been found that the sea surface temperature and sea level in the seas around Korea have continued to rise. The rates of change are still reported to be

higher than the global average. This tendency is present in all of the related papers, which leads to there being a high degree of confidence in these observations. Quantitative data for the rates of change in the sea surface temperature and sea level are presented differently according to the data analysis period and region studied, but the rate is relatively high in the East Sea and around Jeju Island, and low in the Yellow Sea.

Changes in water temperature accompanying long-term ocean warming have been reported, and the east Asian winter monsoon influenced the inter-annual fluctuations in sea surface temperature in the Kuroshio recirculation region that occurred in the 1970s and 1980s, while the spring reappearance process was found to be the main influence in the 1990s. The process of deep water formation in the East Sea has also shown a distinct mid- to long-term change. In contrast to the expansion of the central water volume in the 1990s, a reactivation of the deep water was discovered to occur after 2000. Significant decadal variations in heat capacity in the upper layer and in the characteristics of the water at intermediate depths have also been reported. In the Yellow Sea, trends in the vertical stratification of the water have been described along with the rise in water temperature, and in the Yellow Sea and East China Sea, the mid- to long-term water temperature fluctuations in the decadal time-scale have been confirmed: these can be explained by changes in air-sea heat transport and the wind. Due to the limitations of the data, it is judged that there is only medium confidence in this mid- to long-term variability.

The frequency of extreme phenomena in Korean

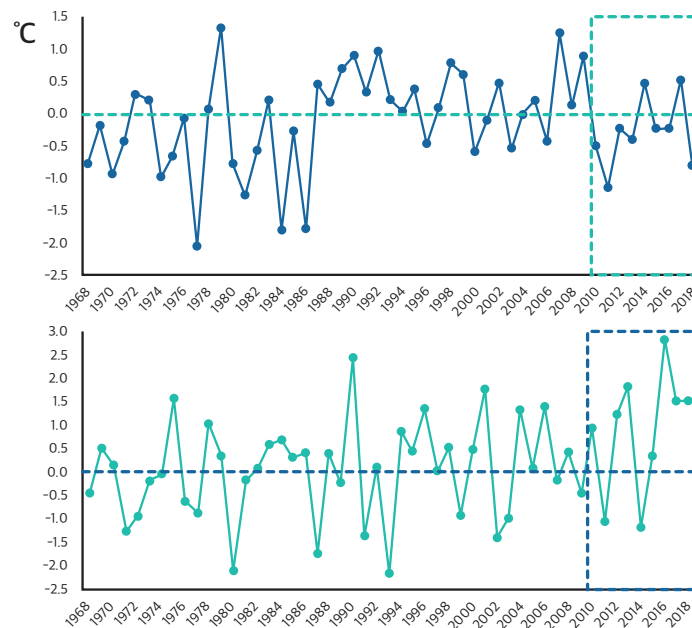


**Fig. 3.1. Trends in mean sea surface temperature anomalies in February (top) and August (bottom) from 1968 to 2017 (MOF, 2019).**

waters has increased (Figure 3.1). In particular, the IPCC’s “Special Report on the Ocean and Cryosphere (2019)” stated that extreme sea surface temperatures—meaning temperatures  $2^{\circ}\text{C}\sim 7^{\circ}\text{C}$  higher than the average—appeared in the East China Sea in 2016, and in the Yellow Sea and the East Sea in 2017.

In terms of ocean biogeochemical changes, there is high confidence that ocean acidification is continuing despite the results of some short-term studies. On the other hand, changes in nutrients have been shown to increase the nitrate concentration and the ratio of nitrogen and phosphorus at the sea surface in the northwest Pacific Ocean, including the Korean seas. However, the cause of this was found to be the flow of nitrogen oxides into the atmosphere due to the rapid industrialization of neighboring countries rather than climate change.

It has been suggested that there have been changes in the cluster structure and geographic distribution of marine species in parts of the East Sea. This observation results from the lack of global observational data and

long-term changes in marine ecosystems. Biological reactions to environmental changes are timed and complex. It is considered that the ocean biological changes caused by climate change can be inferred if the “National Marine Ecosystem Comprehensive Survey” data, which has been operating in all regions of the Korean waters since 2015, is accumulated.

### 3.3. Cryosphere

Temperatures in the Arctic have been rapidly increasing (solid agreement). Arctic warming can cause cold air outbreaks over east Asia and North America (limited agreement). Recently, there has been a clear decline in the area and thickness of sea ice in the Arctic (solid agreement). The area of sea ice in the Antarctic has been increasing, but this increase has slowed since 2015 (intermediate agreement).

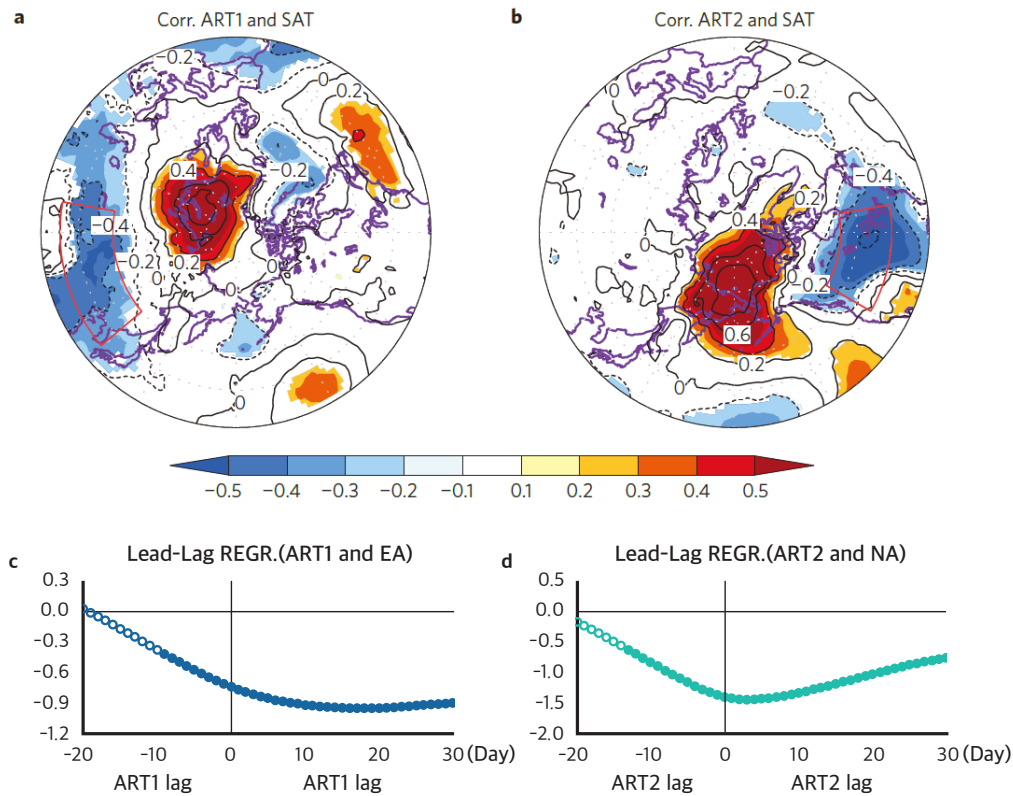


Fig. 3.2. Relation between mid-latitude temperature changes and Arctic temperature (Kug et al., 2015).

Observation and reanalysis data indicate that there was a rise in the annual mean surface temperature in the Arctic from 1980 to 2015, especially in winter. Increases in heat and moisture transport to the Arctic from mid-latitudes, Arctic sea ice reduction, and an associated increase in downward longwave radiation all contributed to the rapid Arctic warming. In contrast, in Antarctica, the temperature did not show any clear trends and there were large spatial and temporal variabilities.

In contrast to the marked sea ice decline and temperature rise in the Arctic, cold air outbreaks have been more common in east Asia and North America in recent winters. This is referred to as “Warm Arctic and Cold Continent”. The cause, impact, and prediction of “Warm Arctic Cold Continent” is in an area of active research. Many studies have suggested that the rapid

Arctic warming and sea ice decline are leading to these cold air outbreaks by modulating the atmospheric circulation (Figure 3.2); however, other results have shown that the recent Arctic warming and cold mid-latitudes are due to internal variability within the climate system rather than a forced response.

In the Arctic, Pacific summer water was widely distributed in the Chukchi Sea in 2012, but the amount diminished with time, and, in 2017, the water mass had shrunk to its smallest value. Pacific winter water also covered the smallest area in the Arctic in 2017, but this water became gradually more dominant by 2018. Overall, from 1980 to 2015, the temperature of water masses in the Chukchi Sea region at depths of 60 m to 80 m increased by 0.5°C per decade. Salinity decreased at a rate of 0.5 psu. The disintegration of ice shelves in west Antarctica has not occurred steadily, but, rather, has occurred episodically and discontinuously. It

appears that the melting of ice is greater when a warm water mass intrudes onto the continental shelf. On the whole, the sea surface temperature in the Arctic is increasing gradually, whereas, in the Southern Ocean, it has been decreasing with time. However, sea surface temperature trends were determined by reanalysis data and, thus, have a high degree of uncertainty, thus warranting more accurate quantification through observation.

From 1979 to 2018, the Arctic sea ice area markedly decreased in all seasons, showing trends of  $-1.6 \pm 0.5$ ,  $-8.1 \pm 1.3$ ,  $-9.3 \pm 1.8$ , and  $-2.0 \pm 0.7\%$  per decade in spring, summer, autumn, and winter, respectively. The average thickness of the Arctic sea ice has also shown a continuous decreasing trend. The rate of decrease has been lowest,  $-9.5 \pm 1.2\%$  per decade, during the ice-maximum season (spring), and the fastest reduction,  $-22.1 \pm 2.9\%$  per decade, has been in the season when the ice is thinnest (autumn).

In the Southern Ocean, the annual sea ice area has shown a slight increasing trend, but since 2015 there has been a substantial reduction in Antarctic sea ice that has compensated for the previous increase. In comparison to the period 1979~2012 that was reported on last time, the overall upward trend in Antarctic sea ice area during the period 1979~2018 has reduced substantially in summer and autumn. In summer, the upward trend has also weakened by more than two thirds. The largest contribution to this reduction in the Southern Ocean is found in the Ross Sea in summer and autumn; the reduction in the Indian Ocean sector in summer has also contributed. The sea ice thickness has tended to increase slightly.

The mass of the Antarctic ice sheet decreased by 3,000 billion tons between 1992 and 2017, which corresponds to an increase in global sea level of 7.6 mm. About 40% of the total ice sheet mass loss has occurred in the past five years in west Antarctica. Over the 10 years 2009~2017, the rate of mass loss from the Antarctic ice sheet was six times faster than in the

period 1979~1989. Recently, the uncertainty in projections of future sea level rise caused by melting of the Antarctic ice sheet has been substantially reduced by improved understanding of the physics and the stability of ice sheets in relation to the melting and inclination of ice shelves. However, the quality of the observation data is still poor and international cooperation is needed to resolve this problem.

Since 1980, the average temperature of the permafrost in most regions of the Arctic has risen, and the rate of increase has been greater over areas of continuous permafrost than over discontinuous layers of frozen ground. The permafrost temperature has increased by  $0.29 \pm 0.12^\circ\text{C}$  over the past decade. In Antarctica, the permafrost temperature has increased by  $0.37 \pm 0.10^\circ\text{C}$ . Besides this, the thickness of the active layer has increased, especially in southern boundaries where the temperature is higher. The permafrost area is also getting smaller as the permafrost disappears near its boundaries.

The area of snow cover in the northern hemisphere is more than 45 million  $\text{km}^2$  in January and February; this decreases to 3 million  $\text{km}^2$  in August. From 1967 to 2018, the area of snow cover in spring steadily decreased, and snow cover reduction also occurred in autumn; however, the uncertainty in the autumn data is larger than for the spring data. For example, the snow cover area in June decreased by  $13.4 \pm 5.4\%$  per decade, which is equivalent to about 2.5 million  $\text{km}^2$  per decade. As well as the decrease in the area of snow cover, the length of time for which snow persists has also been decreasing. There was a particularly marked decrease over Eurasia between 1920 and 2010. Over the Korean peninsula, from 1980 to 2000, snow depth tended to decrease in general, but since 2000 there has tended to be more variability, and the depth has been increasing at a rate of 0.7 cm per year.

# 4. Information from Palaeoclimate Archive



## 4.1. Introduction

As there is a high demand for the accumulation and establishment of long-term comparative palaeoclimate data at both local and global scales, various climatic proxy data, including terrestrial and oceanic deposits such as fauna and flora fossils and tree rings, as well as man-made artefacts including old records and paintings, are being utilized for the reconstruction of past climates.

However, due to the long time span and low resolution of proxy climate data in comparison with modern observational meteorological data sets, there are clear limitations on the use of proxy data to reconstruct past climate change. Only general palaeoclimatic trends can be reconstructed on the basis of the various proxy data available for Korea.

## 4.2. Pollen

There are well-known consistent results based on pollen and vegetation histories both for the whole globe and for the east Asian region (solid agreement).

Recently, high-resolution and good-quality age-controlled pollen results have been obtained from full-drill core sediments and advanced radiocarbon date measurements. This has allowed the dynamic response of vegetation to climate change in the past to be interpreted in detail.

In particular, a short-term global climate event (the 8.2

ka cold event) and an abrupt climate event related to the east Asian monsoon (the 4.2 ka drought) were identified for the Republic of Korea (South Korea) based on high-resolution pollen records obtained from late Quaternary sediments. Moreover, the history of climate variation and vegetation change over the past 50,000 years (since the late Pleistocene) has been revised on the basis of pollen records obtained from marine sediments in the East Sea.

Under the cold and dry climate conditions of the late Pleistocene, subalpine conifer forests and open grasslands predominated on the mountain slopes and in the lowlands of Korea, respectively. The sea-level rise that occurred during the early to mid-Holocene had a great influence on the climate and plant ecology.

Based on the high-resolution pollen record obtained from the west coast wetland sediments, it was the first recognized that an abrupt change to a cold and dry climate occurred during the early Holocene (8,300~8,000 years BP) across the Korean peninsula. This event aligns well with the abrupt 8.2 ka cold event that affected the northern Hemisphere as a whole. During the early-mid Holocene (8,000~6,500 years BP), broad-leaved deciduous and evergreen forests flourished across the Korean peninsula, whereas the dry-tolerant grasses declined. These trends continued until the Holocene climatic optimum, which was characterized by a warm and wet climate due to an enhanced east Asian summer monsoon.

## 4.3. Animal

This analysis was mainly conducted in the limestone area of Gangwon Province, where many animal fossils dating mainly from the latter part of the Pleistocene can be found. This analysis is deemed to be beneficial to an overall understanding of the environment and climate change during the Quaternary in Korea (solid agreement).

There are about 20 cave sites belonging to the upper Pleistocene; the characteristics of animal remains excavated from the sites dating from this period can be summarized as follows. The first concerns the occurrence of different animals. More than 50 species of animals from this period have been reported, many more than the from the earlier middle Pleistocene period (30 species): the increase in carnivores is the most noticeable, from large carnivores such as tigers (*Panthera tigris*), lions (*Panthera cf. Leo*), and bears (*Ursus arctos*) to medium-sized animals such as hyenas (*Hyaena sp.*), wolves (*Canis lupus*), foxes (*Vulpes vulpes*), raccoons (*Nyctereutes sp.*), and badgers (*Meles meles*). This increase indicates that the climate of this period was temperate and coexisted with forest.

Meanwhile, the latter part of the upper Pleistocene is characterized by the existence of mammoths (*Mammuthus primigenius*), woolly rhinoceroses (*Coelodonta antiquitatis*), and musk deer (*Moschus moschiferus*), which are considered to be animals that represent the cold climate of the last glacial maximum (LGM). However, the relationship with human activity shows that the main target of hunting at that time was deer: according to a quantitative comparison of the fossil species, more than 90 percent of all animal fossils have been found to be skeletons of deer.

The most significant change in fauna occurred during the transition from the Pleistocene to the Holocene. Many animals disappeared during the Holocene, especially the large animals found during the cold LGM. The Holocene fauna, usually found in shell middens,

and some caves, existed in a warm climate and consisted of medium or small animals. In particular, medium-sized carnivores lived until the Neolithic and the Bronze Age. Meanwhile, the extinction of large mammals such as mammoths and woolly rhinoceroses is a good indicator of the climate change that occurred.

#### 4.4. Tree ring

The climate characteristics that are presented, which were reconstructed using cellular anatomy and tree-ring  $\delta^{18}\text{O}$  chronologies, were determined using proven published methods (solid agreement).

In the last three years, no studies on the reconstruction of paleoclimates using tree-ring width data have been published. On the other hand, several reports verifying the potential of time series based on cell-size (referred to hereafter as cellular anatomy chronology) and  $\delta^{18}\text{O}$  data (hereafter tree-ring  $\delta^{18}\text{O}$  chronology) from each ring for reconstructing paleoclimates have been published. It has been established from cellular anatomy and  $\delta^{18}\text{O}$  tree-ring chronologies that paleoclimates can be reconstructed; in addition, different climatic signals can be identified from ring-width chronology. Such findings allow various seasonal climates to be reconstructed if cellular anatomy and tree-ring  $\delta^{18}\text{O}$  chronologies, together with ring widths, can be applied to the climate reconstruction. Several chronologies based on cellular anatomy or  $\delta^{18}\text{O}$  tree-ring data have shown higher correlations with climate characteristics than ring-width chronology has.

The first Korean cellular anatomy chronologies were established based on vessel areas of Mongolian oak (*Quercus mongolica*) at high elevations on Mt. Songnisan. Using analysis of the correlation between these chronologies and climate factors, it was found

that the chronologies were able to provide a reasonable proxy for the reconstruction of winter precipitation based on the significant positive correlation between the two variables. The first domestic tree-ring  $\delta^{18}\text{O}$  chronologies were established for spreading yew (*Taxus cuspidata*), Korean pine (*Pinus koraiensis*), Korean fir (*Abies koreana*), and *Quercus mongolica* found at high altitudes on Mt. Jirisan. In contrast to the vessel-area chronologies, the  $\delta^{18}\text{O}$  tree-ring chronologies showed positive correlations with spring

and summer temperatures, whereas there was a negative correlation with precipitation during the same period (Figure 4.1). Furthermore, the  $\delta^{18}\text{O}$  chronologies showed significant negative correlations with precipitation between May and July in western Japan. These chronologies, therefore, can act as a reliable proxy for reconstructing the east Asian monsoon. As a result of these studies, a 235-year (1780~2014) cellular anatomy chronology and a 152-year (1864~2015)  $\delta^{18}\text{O}$  tree-ring chronology have been successfully

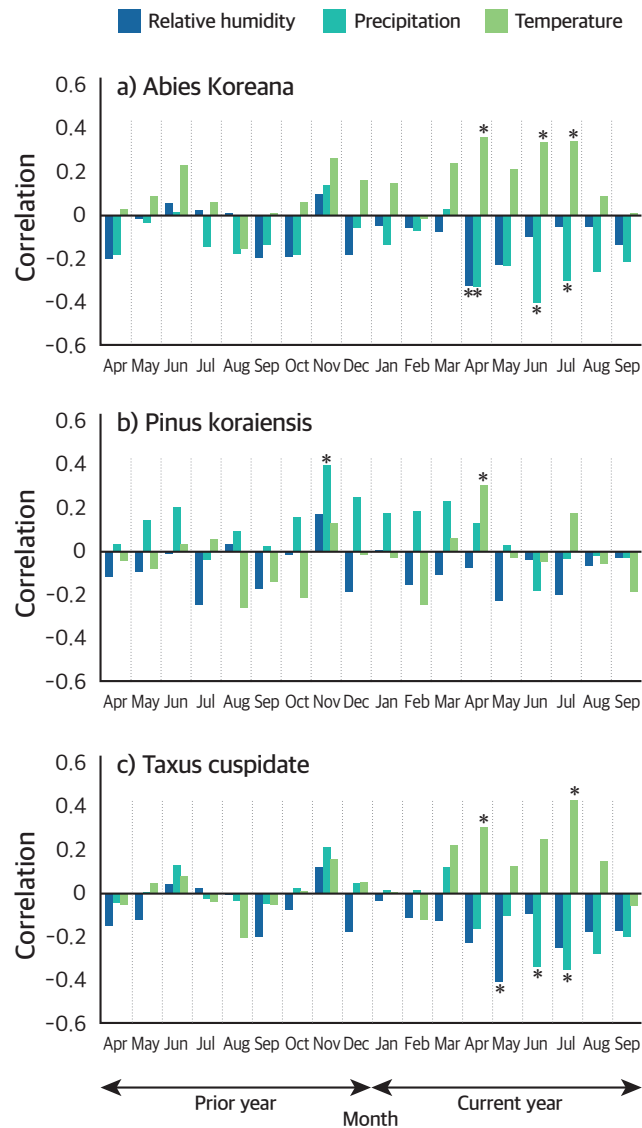


Fig. 4.1. Correlation of (a) *Abies koreana*, (b) *Pinus koraiensis*, and (c) *Taxus cuspidata* tree-ring  $\delta^{18}\text{O}$  chronologies with relative humidity, precipitation, and temperature from April of the previous year to September of the current year (Seo et al., 2019).

## 4.5. Old documents

The results of earlier studies were mere statistics that used simple record numbers. However, studies published over the past five years have produced concrete research results based on sophisticated research methods that consider various factors (solid agreement).

Many Korean historical records, such as “The Annals of the Joseon Dynasty”, “The Annals of Seung-jeongwon (Seongjeongwon Ilgi)”, and the “Oegwan Guansu Diary”, can be utilized for the reconstruction of climate change and weather-related disasters in Korea.

The number of clear days was higher than today and the number of cloudy days was lower. The number of days with rain varies greatly—from 19.5 days prior to the 1710s to 63.8 days after this. The annual average precipitation recorded between 1771 and 1800 was 941.5 mm, which is 35.1% less than the present-day annual average precipitation (1,450.6 mm). The number of days with precipitation during the period 1771~1800 was higher than in other periods, and the climate prior to 1770 was relatively dry. Numerous records related to the Ritual for Rain (or Rain Calling Ceremony) also confirm the frequency of dry periods from 1623 to 1770. These trends seem to be due to the fact that the climate on the Korean peninsula, including Seoul, was greatly affected by the Little Ice Age. Snowfall records for October during the periods 1623~1650, 1711~1740, and 1771~1800 also indicate the occurrence of cold climate episodes.

During these cold periods, snowfall began earlier than usual and continued to later in the spring, indicating that winters were longer and colder. Records of drought and other drought-related events, including rain ritual records, indicate that drought was more common in the earlier period of the Joseon Dynasty than later in the dynasty. Records of the date of the

first frost show that this date gradually became later from the 17<sup>th</sup> to the 19<sup>th</sup> century, and the number of frost per month was higher than the present-day average. This may indicate that the climate conditions of the 17<sup>th</sup> century were colder than those of the 19<sup>th</sup> century—the later period of the Joseon Dynasty.

Analysis of historical records from the Joseon Dynasty, thus, shows that the Little Ice Age affected Korea during the 17<sup>th</sup> century.

# 5. Carbon and Other Biogeochemical Cycle



## 5.1. Introduction

The content summarized in this section concerns mostly local, sporadic, and short-term observations and process-level studies. In recent years, some modeling and algorithm development, as well as comparative validation and studies based on machine learning, have begun to fuse research and modeling. Based on these preliminary results, we summarize the importance, trends observed in, and level of understanding of the carbon cycle and other major biogeochemical feedbacks in the Korean Peninsula, east Asia, and the polar regions.

from wetland ecosystems will increase further with increasing CO<sub>2</sub> and a warmer climate (intermediate agreement).

## 5.2. Carbon cycle

Increased CO<sub>2</sub> emissions due to fossil fuel combustion and changes in land use are the main contributors to the observed increases in the atmospheric CO<sub>2</sub> concentration (solid agreement). Climate change and lack of nutrients will partially offset the terrestrial ecosystem's carbon uptake caused by increasing atmospheric CO<sub>2</sub> (solid agreement). Physical and biogeochemical carbon cycles on land will continue to respond to increases in atmospheric CO<sub>2</sub> and climate change during the 21<sup>st</sup> century (solid agreement). The CH<sub>4</sub> concentration, which had been stable for a decade since the early 1990s, has increased since 2007 (intermediate agreement). CH<sub>4</sub> emissions

In Korean forest ecosystems, the decline in forest area has slowed down in recent years; however, with the aim of increasing the degree of self-sufficiency in wood, the amount of logging has been increasing. The impact of thinning on carbon accumulation differs according to the amount of thinning, the method used to collect and thin lumber, and the follow-up management methods. Due to the aging of old-growth forests and disturbances such as pine nematodes and forest fires, the role of forest ecosystems as CO<sub>2</sub> sinks is changing and their sink capacity is expected to decrease. It has also been reported that the management of forest soils during the dormant winter period has a significant impact on carbon emissions. Forest ecosystems are estimated to absorb approximately 3% of anthropogenic CO<sub>2</sub> emissions, but the amount of forest carbon accumulation is predicted to decrease in the future. However, it is encouraging that various in-depth studies and the linking of observation and modeling in the 5<sup>th</sup> and 6<sup>th</sup> national forest resource surveys are being employed for future forest management strategies and in proposals for the planting of new species. Furthermore, research is in progress on the effects on the carbon cycle of the management of saw timber-stage forests and of forest work carried out soon after reforestation.

It has been reported that Korean agricultural ecosystems are CO<sub>2</sub> sources rather than being CO<sub>2</sub>

neutral. To evaluate whether agricultural land is a source or sink of greenhouse gases (GHGs, including CO<sub>2</sub>), the entire year (including the period when there is no cultivation) must be considered along with the amount consumed after being transported outside agricultural lands after harvesting.

The reason why agricultural ecosystems are generally recognized as being CO<sub>2</sub> neutral is that the harvest is either consumed or decomposes and then released back into the atmosphere. Both single and double cropping of rice and barley have been reported as being sources of CO<sub>2</sub> and CH<sub>4</sub> on an annual basis. Intermittent irrigation with midsummer drainage (the usual management practice used for rice cultivation in Korea) leads to increased N<sub>2</sub>O emissions, and thus is considered to be a source of GHGs. However, agro-ecosystems such as apple orchards have been reported to function as CO<sub>2</sub> sinks. For an accurate evaluation and to design mitigation strategies, continuous long-term observations over whole life-cycles are required.

Meanwhile, the CH<sub>4</sub> emissions from rice fields are reported to have been underestimated, necessitating the re-evaluation of these emissions. The re-evaluated CH<sub>4</sub> emissions from areas of rice cultivation in individual cities and counties were made by using improved water-management correction factors together with data from the 2010 Census of Agriculture, Forestry and Fisheries and the 2006 IPCC guidelines for evaluating CH<sub>4</sub> emissions (Figure 5.1). The re-evaluated methane emissions due to rice cultivation were  $380 \pm 74$  kg CH<sub>4</sub> ha<sup>-1</sup> yr<sup>-1</sup>, which is significantly greater than the reported emissions that were calculated using the national emission factors without water-management correction.

In the case of freshwater ecosystems, the organic and inorganic carbon contained in rivers amounted to 905 Gg C yr<sup>-1</sup> (equivalent to 1/4 of the estimated net ecosystem productivity of forests in Korea). For the rivers and lakes in the Han River basin, large amounts

of CO<sub>2</sub> and CH<sub>4</sub> were discharged from the lower part of the basin and from tributaries that are heavily affected by sediment and by sewage treatment plants due to the accumulation of large amounts of organic matter. Organic matter deposited in numerous dams and small-scale agricultural reservoirs has a two-sided effect (i.e., it acts as a store of carbon but also as a GHG emission source). However, it is impossible to predict the carbon balance of the lacustrine environment in Korea based only on the results available so far. In addition to making basic surveys for accurate carbon balance prediction in the future, continuous and systematic field surveys are needed to properly understand changes in GHG emissions due to changes in reservoir life or to seasonal changes such as drought or flooding.

In polar ecosystems, GHG feedbacks in tundra

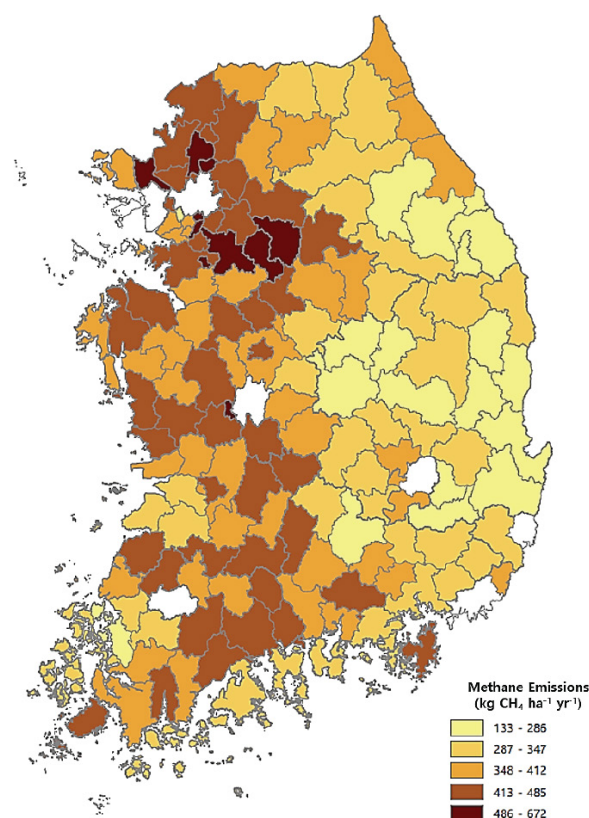


**Fig. 5.1. Re-evaluated CH<sub>4</sub> emissions per unit area of rice paddy across Korea based on data from the 2010 Census of Agriculture, Forestry and Fisheries (Choi et al., 2018)**

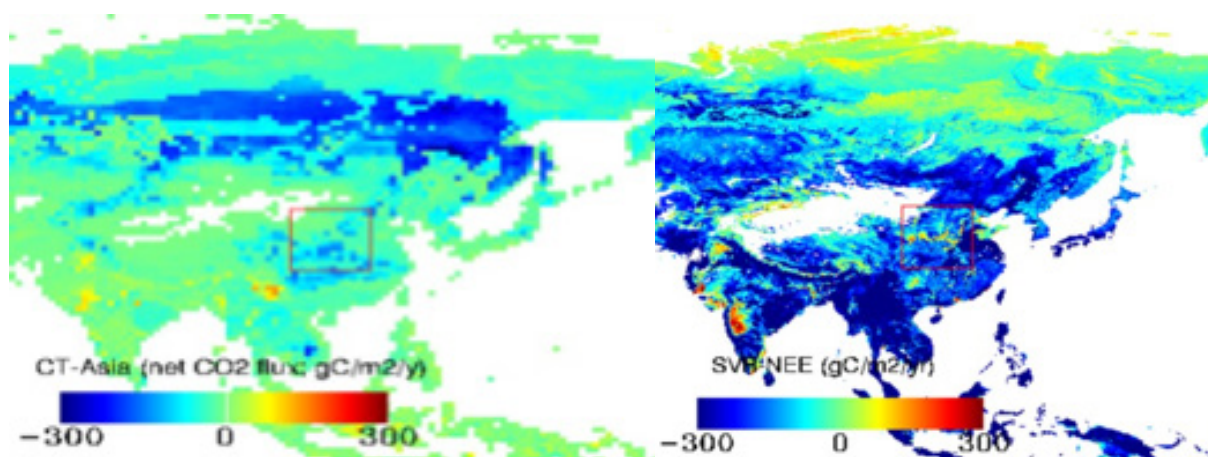


Fig. 5.2. Asian CarbonTracker's  $1^\circ \times 1^\circ$  net biome productivity (left) and Support Vector Regression-based  $0.25^\circ \times 0.25^\circ$  net ecosystem exchange (NEE) (right) (Kim et al., 2018).

ecosystems including permafrost (i.e., land that has been frozen for more than two years in a row) due to warming in the Arctic have been reported to be very important to climate change prediction. The results of research conducted over the past decade in the Arctic, Alaskan tundra ecosystems, and the Antarctic by Korean researchers (including the Polar Research Institute) have been included in the report. According to recent observations from wet tundra areas in the Arctic and Alaska, changes in topography and precipitation patterns are expected due to the thawing of permafrost. This will result in changes in soil moisture distribution and, in turn, will have a significant impact on carbon exchange. If the permafrost melts, the soil will get wetter and the decomposition rate of old carbon will increase but this effect may be offset if new dry areas emerge.

The Asian CarbonTracker tracks carbon globally and focuses on Asia. As an independent system for monitoring and evaluating the effects of  $\text{CO}_2$  emissions and mitigation activities, the Asian CarbonTracker is in good agreement with observations. The  $\text{CO}_2$  concentration has increased since 2001, and its distribution varies regionally due to fluctuations in absorption and emission. Emissions are due to the combustion of fossil fuels, which has increased almost

linearly but with small interannual variations. As a result of the optimization of data assimilation parameters and the construction of a new assimilation system for airborne and satellite data, improved estimates of surface  $\text{CO}_2$  flux have been presented for comparison with inverse modeling and observation-based estimates (Figure 5.2). It is pointed out that more ground observation sites are needed in Asian regions where there are large uncertainties, along with the importance of making observations in Siberia.

### 5.3. Other biogeochemical cycle

The  $\text{N}_2\text{O}$  concentration has increased at a rate of  $0.73 \pm 0.03 \text{ ppb yr}^{-1}$  over the past 30 years (intermediate agreement).  $\text{N}_2\text{O}$  emissions from soil will increase due to increasing nutrient and dependence on nitrogen fertilizers (intermediate agreement). Due to human activities, concentrations of aerosols, including GHGs, reactive gases and secondary products, will increase significantly, leading to a decrease in air quality at the

The biogeochemical cycle of nitrogen has already exceeded a limit that should not be crossed. The  $N_2O$  concentration has increased by 20% above the pre-industrialization level, with the use of chemical fertilizers and livestock manure being the main causes. Korean studies related to the nitrogen cycle have been conducted mainly to estimate  $N_2O$  emissions from farmland and to develop national emission factors according to IPCC guidelines.

Wetlands serve as a link to the biochemical cycles of carbon (C) and nitrogen (N), and contribute to the GHG balance. However, little on-site measurement data has been gathered. Agriculture is estimated to account for 2/3 of the annual  $N_2O$  emissions from human activities. The  $N_2O$  emissions from rivers and lakes, which are highly affected by farmland runoff and urban sewage, have increased significantly, reaching 10% of the anthropogenic release of  $N_2O$ . According to the results of a small number of field surveys conducted on the  $N_2O$  emitted from rivers and lakes in the Han River basin,  $N_2O$  concentrations were relatively high in dammed sections with high concentrations of N and also in downstream sections of the Han River. The effluent from sewage treatment plants was identified as the main source of  $N_2O$ . However, further studies based on continuous monitoring are needed to ascertain the environmental conditions under which  $N_2O$  is emitted from river water or sediments.

Regarding the cycles of short-lived climate pollutants resulting from the increase in urban forests, accurate diagnosis of biogenic volatile organic compounds (BVOCs) is needed along with an understanding of their impacts on the production and feedback mechanisms of ozone and aerosols. Due to the paucity of observation data, the emission rates of BVOCs are calculated using models, and their concentration, emission, and photochemical processes are poorly understood. As part of research and countermeasures to reduce fine dust, national

and local governments in Korea are planning to expand urban forests, which is considered to be an effective means of mitigating climate change. However, it is difficult to predict the effect of feedbacks because BVOC emissions will increase when drought or high temperature persist. BVOCs can easily produce ozone and fine dust when mixed with  $NO_x$  or  $SO_2$  emitted from the surroundings. Therefore, comprehensive and long-term observations of biogeochemical cycles of reactive C, N, and sulfur (S) compounds are needed: this requires integrating ozone, fine dust, air quality and climate change to establish scientific policies.

# 6. Clouds and Aerosols



## 6.1. Introduction

This report summarizes research papers on clouds and aerosols published in 2014~2019. As in the previous report, only the key papers on the subjects of clouds and aerosols in Northeast Asian regions including the Korean Peninsula, authored by the researchers affiliated in Korean institutions and the Korean researchers working in foreign research institutions are summarized. Table 6.1 lists the number of papers on each subject group.

**Table 6.1. Number of papers on the subject of clouds and aerosols in the northeast Asian region authored by researchers at Korean and foreign institutions. The numbers in parentheses indicates foreign institutions.**

Subject	International	Domestic	Total
Clouds	30(4)	6	36
Aerosols	75(10)	1	76
Cloud-Aerosol Interactions	17(5)	2	19
Radiative Forcing and Effect Radiative Forcing	20(12)	0	20
Processes underlying Precipitation Changes	4(3)	1	5

## 6.2. Clouds

Discussions of the confidence level in relation to cloud observation studies is premature since the number of these studies was so low (limited agreement).

Most studies on in-situ measurements of clouds have analyzed the data from airborne measurement campaigns outside Korea. Airborne measurements of liquid, mixed-phase and ice clouds in various regions were analyzed in order to study the effects of the following: entrainment and mixing of dry air from above the cloud tops on cloud microphysics, the aspect ratio of ice crystals as a function of temperature, ice crystal formation by homogeneous freezing in continental deep convective clouds, and the microphysical properties of stratocumulus clouds over the Southern Ocean. Also notable were remote sensing studies of clouds using a cloud radar that investigated the relationships between radar reflectivity and cloud water content, and between radar reflectivity and rain rate.

Numerical modeling studies on clouds have focused mostly on the improvement of calculations of cloud microphysical processes in cloud-resolving models. These include: improvement of cloud droplet activation process parameterization, consideration of turbulence enhanced collision efficiencies, and improvement of auto-conversion process calculations. Notable studies have included Lagrangian cloud model studies-this became a very active area of research due to the advantage of tracking down the growth of individual cloud drops. Parameterization of ice nucleation process by silver iodide (AgI particles) was developed and implemented in the WRF model to study the effects of AgI seeding on precipitation enhancement in the mountainous Gangwon region.

## 6.3. Aerosols

Aerosol scattering and absorption coefficients, as well as concentrations, measured at Gosan, Jeju-do, and Anmyeon were similar to those for other regions in Asia with similar pollution levels but were much higher than those for clean background regions around the world. (solid agreement). There are not many modeling studies that compare the results of aerosol source apportionment in Korea (limited agreement).

As in the previous report, aerosol measurement studies were the most active field of study in this report. Especially notable was the active international collaboration in comprehensive measurement campaigns. Aerosol scattering properties have been continuously measured at Gosan, Jeju-do, which is a background station. In addition, measurements have been made at western coastal sites as well as in Seoul, where pollution sources and transportation pathways were identifiable. Changes in aerosol optical properties due to secondary aerosol formation during the transport of pollution from China were studied. Comprehensive measurements of aerosol and cloud condensation nuclei (CCN) on the ground, and using research vessels and aircraft were made during the Megacity Air Pollution Studies-Seoul (MAPS-Seoul) and Korea-US Air Quality (KORUS-AQ) campaigns. Long-term measurements of aerosols and CCN at various locations around the world, including Seoul, were reported in a paper resulting from international collaboration. Also notable were polar aerosol studies. Long term ground/satellite remote sensing measurements of aerosol distribution revealed that during 2004~2014, aerosol optical depth increased but particles sizes decreased in China; however, no such trends were found in Korea.

Several regional/global atmospheric chemistry studies on aerosol sources and transport in Korea revealed that the occurrence of severe pollution in

recent years was mostly due to the transport of large amounts of polluting aerosols emitted in China; however, on normal days, the contribution of local Korean sources was significant. Much attention was given to the transformation of gaseous pollutants such as SO<sub>2</sub> and NO<sub>x</sub> into secondary aerosols by some chemical reactions. Studies on dust have slightly reduced in recent years. Coincidentally, the number of dust events has reduced and it has been estimated that changes in wind fields and mesoscale pressure patterns have somehow weakened the strength of dust transport to the Korean peninsula.

---

#### 6.4. Aerosol-cloud interaction

There have been various recent studies on aerosol-cloud-precipitation interactions, but the number of studies is still small (limited agreement). Studies related to modeling of these interactions were comparatively more numerous

Aerosol-cloud interaction studies include feedback mechanisms that involve not only aerosols and clouds but also precipitation and interactions with the boundary layer processes. At the climate scale, aerosol effects on monsoon circulation and hydrological cycles have been the main focus. Since aerosol-cloud-precipitation interactions involve non-linear feedback mechanisms and complex responses to changes in aerosol concentration, quantitative assessment of indirect aerosols has been very difficult despite continuous advances in measurement capabilities. However, this has been a very active area of research in northeast Asia, where aerosol pollution has increased very quickly in recent decades along with the rapid industrialization of China.

Numerical modeling studies have focused on the

effects of aerosols on cloud and precipitation development and on assessment of the effects of aerosol distribution changes at the global scale. Precipitation responses to changes in aerosol concentration have not been consistently in one

direction. It has been reported that, from a general circulation perspective, the increase in anthropogenic aerosols in east Asia has affected the radiation budget in this region and weakened the monsoon circulation (Figure 6.1).

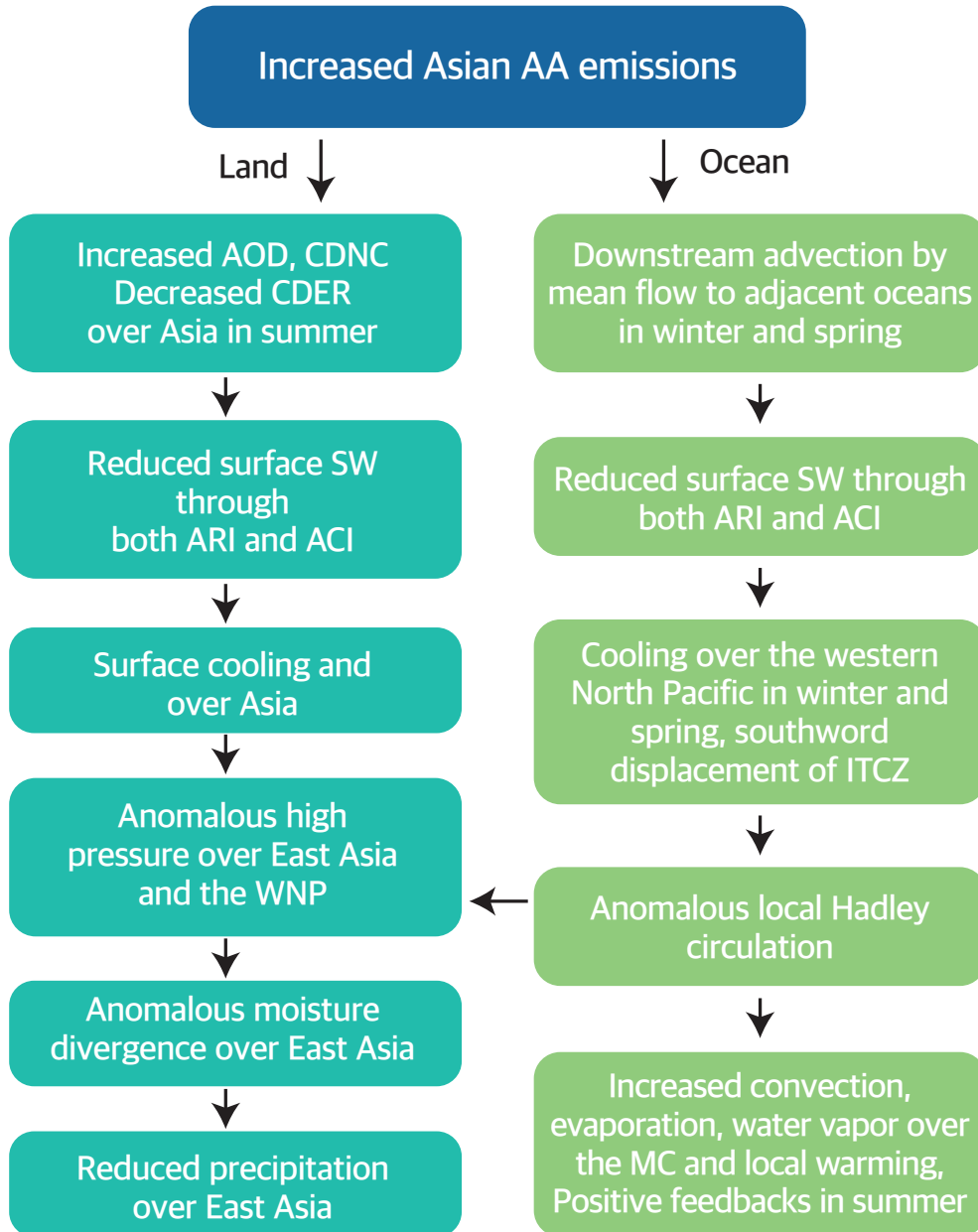


Fig. 6.1. Schematic diagram showing the effects of artificial aerosols on the summer monsoon and precipitation mechanisms over east Asia (Dong et al., 2019).

## 6.5. Radiative forcing and effective radiative forcing

Given the distribution of aerosols, the results of radiative forcing at Jeju are important. However, there are not many related studies (intermediate agreement). Several studies have produced similar results on changes in dust radiative forcing; however, in some cases, the quantitative results do not agree (intermediate agreement). From a global perspective, the understanding of cloud radiative effects has improved in recent decades (intermediate agreement).

Based on analyses of 2006~2012 satellite data and model simulation results, it has been estimated that the amount of atmospheric heating and cooling of the Earth's surface resulting from biomass burning were both twice as great as that due to dust particles. It has also been reported that springtime surface radiation reduced by  $10 \text{ Wm}^{-2}$  during the period 1980~2012. The radiative efficiencies of dust, mixed particles, and anthropogenic aerosols were, respectively:  $-101.0 \text{ Wm}^{-2} \text{ t}^{-1}$ ,  $-112.9 \text{ Wm}^{-2} \text{ t}^{-1}$ , and  $-98.3 \text{ Wm}^{-2} \text{ t}^{-1}$  at the surface;  $-42.3 \text{ Wm}^{-2} \text{ t}^{-1}$ ,  $-22.5 \text{ Wm}^{-2} \text{ t}^{-1}$ , and  $-39.8 \text{ Wm}^{-2} \text{ t}^{-1}$  at the top of the atmosphere; and  $58.7 \text{ Wm}^{-2} \text{ t}^{-1}$ ,  $90.3 \text{ Wm}^{-2} \text{ t}^{-1}$ , and  $58.5 \text{ Wm}^{-2} \text{ t}^{-1}$  in the atmosphere. It has been argued that a mixture of dust and anthropogenic aerosols could stabilize the atmosphere by heating the atmosphere but cooling the surface, but thereby worsening the pollution. AEROSOL ROBOTIC NETWORK (AERONET) data indicated that radiative forcing was directly determined by the aerosol amount but that the radiative efficiency varied depending on the aerosol types and surface albedo. The cooling at the top of the atmosphere and heating in the atmosphere were also confirmed by numerical modeling studies.

## 6.6. Processes of precipitation change

Aerosol-cloud microphysics-dynamics feedback mechanisms have become a subject of great interest in recent years. It is thought that delayed and reduced precipitation due to an increase in aerosols may result in greater latent heat release from freezing as well as greater evaporative latent heat absorption. This could affect the thermodynamics and dynamic structures of clouds and eventually lead to changes in convection and the structure of cloud systems.

Aerosol-cloud-precipitation interactions are known to be very important to improvements in climate change prediction but only a few researchers have worked on this issue in Korea. Meaningful contributions may come only after Korean institutions are well equipped with basic measurement instruments and carry out well-organized, continuous and reliable measurements.

# 7. Anthropogenic and Natural Radiative Forcing



## 7.1. Introduction

The radiative forcing (RF) concept has been used for evaluating the strength of the various mechanisms affecting the Earth's radiation balance and thus causing climate change. It is unequivocal that anthropogenic increases in greenhouse gases (GHGs) related to human activities have substantially enhanced the greenhouse effect, and the resulting RF continues to increase. Aerosols partially offset the forcing due to GHGs and dominate the uncertainty associated with the total anthropogenic driving of climate change. This section summarizes the RF over east Asia and Korea in terms of both natural and anthropogenic components. Owing to the small number of recent studies on anthropogenic and natural RF, the uncertainty in the amount of RF is described qualitatively.

## 7.2. Tropospheric ozone

The surface-level ozone concentration in east Asia and Korea has been consistently increasing due to increased precursor emissions. The occurrence of high-ozone episodes has also increased (solid agreement).

Tropospheric ozone ( $O_3$ ) is a major GHG and an important air pollutant that is strongly influenced by changes in the temporal and spatial distribution of precursor emissions, and is also known to be highly sensitive to regional climate change. Unlike the United States and Europe, the surface  $O_3$  concentration in east Asia continues to increase due to increased precursor emissions. In Korea, the number of days on which an  $O_3$  advisory was issued increased from 22 days

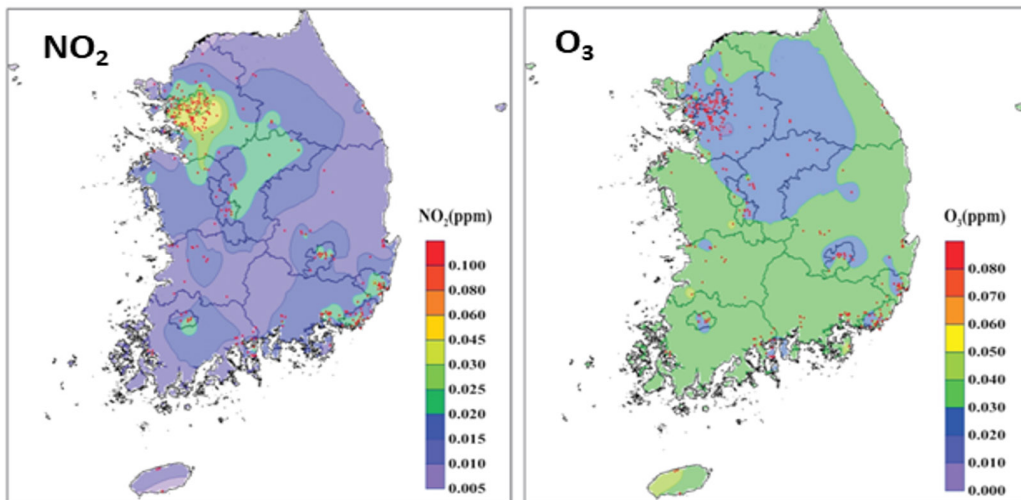
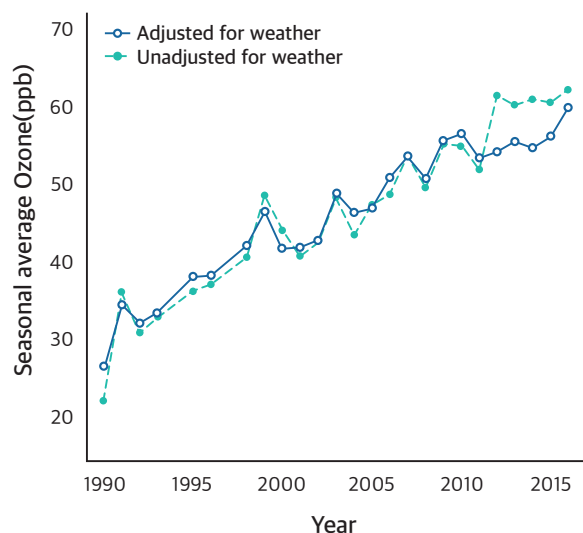


Fig. 7.1. Annual mean concentrations of  $NO_2$  and  $O_3$  in surface air in 2017. Red dots indicate air pollution monitoring sites (NIER 2018).

in 2007 to 66 days in 2018, and the number of O<sub>3</sub> warnings also increased by nearly 10 times from 52 in 2006 to 489 in 2018.

In Korea, the concentration of O<sub>3</sub> is lowest in winter (November to February) and highest in spring (April–June). In summer (July–August), the concentration is lower than in spring due to an increase in precipitation and a decrease in solar radiation. The O<sub>3</sub> concentration is also highest between 2 pm and 5 pm, which is when photochemical reactions occur due to high temperatures and intense solar radiation; the lowest concentration occurs between 7 am and 8 am. Figure 7.1 shows the spatial distribution of the annual mean O<sub>3</sub> concentration; it is clear that the pattern is the opposite to that for the spatial distribution of NO<sub>2</sub>. In particular, O<sub>3</sub> concentrations are relatively low in metropolitan areas, where air pollutants are concentrated.

Modeling studies have reported that the long-term increase in O<sub>3</sub> concentration in east Asia is influenced by variability in meteorological fields and that the



**Fig. 7.2.** Daily maximum summertime 8-hour O<sub>3</sub> concentrations from 1990 to 2016 in Seoul. The solid line indicates the observed O<sub>3</sub> trend, and the dotted line indicates the O<sub>3</sub> trend without the influence of the weather (Kim et al. 2017).

increase in O<sub>3</sub> in urban areas is also significantly affected by the O<sub>3</sub> titration effect of the NO<sub>x</sub> emitted from automobiles (Figure 7.2).

In addition, the decrease in PM<sub>2.5</sub> mass due to strong regulatory policies is contributing to the increase in the O<sub>3</sub> concentration in China. Therefore, detailed monitoring of emissions of aerosols and O<sub>3</sub> is required in relation to future regional climate change.

### 7.3. Anthropogenic radiative forcing

The concentrations of CO<sub>2</sub> and methane observed in Korea are about 5 ppm, 8 ppm, and 100 ppb higher, respectively, than the global mean concentrations, indicating that the resulting RF is similar to or slightly higher than the global RF (solid agreement). The RF due to ozone is expected to increase continuously because the total ozone concentration in the atmosphere has been steadily increasing (solid agreement).

The global mean RF due to increasing GHG concentrations is estimated to be 2.83 (2.54–3.12) W m<sup>-2</sup>. The RF due to CO<sub>2</sub>, which contributes most to this, is 1.86 (1.33–2.03) W m<sup>-2</sup>. The RF due to methane and nitrous oxide is 0.48 (±0.05) W m<sup>-2</sup> and 0.17 (0.14–0.20) W m<sup>-2</sup>, respectively. The RF due to stratospheric ozone resulting from halocarbons is approximately 0.18 (0.01–0.35) W m<sup>-2</sup>.

Owing to the small number of recent studies on the RF of GHGs in east Asia and the Korean peninsula, it is not easy to produce a quantified analysis at present. However, several studies have revealed that, recently, the mixing ratios of CO<sub>2</sub> and CH<sub>4</sub> have increased by 5 ppm, 8 ppm, and 100 ppb, respectively. The mixing ratio of N<sub>2</sub>O has been similar to the global mean. Consequently, it is considered that, in the Korean

peninsula, the RF due to GHGs is similar to or a little higher than the global mean. Given the continuous global increase in GHG concentrations, it is likely that the RF due to GHGs will increase in East Asia in the future.

The mean total ozone column at Seoul was 325 DU from 1985 to 2018, with the maximum value (361 DU) occurring in March and the minimum (290 DU) in October. Over the course of a year, the total ozone concentration varies by around 71 DU, or 22% of the annual mean value. In terms of long-term changes, the decadal mean total ozone for Seoul was 323 DU in the 1990s and 328 DU in the 2000s—a 5 DU increase. The decadal mean total ozone at Pohang was 309.7 DU in the 1990s and 316.0 DU in the 2000s, meaning that here there was an increasing trend. Despite the regional differences across the Korean peninsula, it is obvious that tropospheric ozone and total ozone in the Korean peninsula is increasing, meaning that the regional RF due to ozone has been enhanced. However, the Arctic ozone hole now often appears unexpectedly, and so the possibility of sudden changes in ozone-related RF in east Asia should not be neglected.

Recent studies have reported that the amount of aerosol RF in east Asia, including the Korean peninsula, is about  $-1 \text{ W m}^{-2}$  to  $-3 \text{ W m}^{-2}$ , which is stronger than the global mean of  $-0.35 \text{ W m}^{-2}$ . This implies that east Asian aerosol pollution is still quite high in spite of the recent decreasing trend. Research during the Korea-US Air Quality (KORUS-AQ) campaign in May-June 2016 reported that the direct RF of the black carbon at the top of the atmosphere was about 1.0 (0.5 - 1.9)  $\text{W m}^{-2}$  and that the variations in this were largely due to regional meteorology. Model simulations using measurements made during the KORUS-AQ campaign revealed that the radiative forcing due to black carbon was  $26 \text{ W m}^{-2}$  -  $39 \text{ W m}^{-2}$  at the surface and  $32 \text{ W m}^{-2}$  -  $51 \text{ W m}^{-2}$  in the atmosphere over east Asia. In recent research, analysis has also been carried out to find the

RF due to organic carbon in east Asia. The magnitude of this is small compared to the influence of black carbon. Since some components of the forcing have unique patterns (e.g., the large absorption of shortwave ultraviolet radiation by brown carbon), more detailed quantitative analysis is required in the future.

---

## 7.4. Natural effect of radiative forcing

The main sources of natural radiative forcing are changes in solar and volcanic activity. The natural radiative forcing due to these two sources is insignificant compared to the anthropogenic effect.

The radiative forcing due to changes in solar is calculated to be  $0.05 \text{ W m}^{-2}$  based on total solar irradiance (TSI) observations made since 1750. Changes in solar activity lead to an enhancement of the Arctic Oscillation in the northern hemisphere troposphere, and potentially affect the relationship between solar activity and ozone.

The radiative forcing due to changes in volcanic activity is estimated to be  $-0.11 \text{ W m}^{-2}$ , but the effects tend to be regional and short term: cases that have global effects are very rare. The eruption of the Eyjafjallajökull volcano in 2010 did have an effect globally and produced a forcing of  $-0.5 \text{ mW m}^{-2}$ , which is still negligible compared to the anthropogenic effect.

---

## 7.5. Emission metrics

Emission metrics are simplified and quantified measures of the response of the climate system to the emission of climate forcers. Among various emission metrics, the Global Warming Potential (GWP) and Global Temperature Change Potential (GTP) are the most common and have been used in numerous

studies to estimate the impact of climate forcers on the Earth's systems.

Since 2010, the GWP has been used in assessments of the environmental impact of the release of GHGs from the construction, energy, and manufacturing industries in Korea. However, only a few studies have focused on the characteristics, limitations, and improvements of emission metrics in Korea.

In recent decades, studies of the characteristics and limitations of emission metrics have been performed around the world. For example, ensemble and multi-model simulations have been conducted to overcome the limitations of the GWP and GTP. As both metrics show consistent regional variations, the spatial patterns obtained using the GWP and GTP are considered to be robust despite the large discrepancies that exist between studies. However, the use of GWP and GTP has fundamental limitations since these metrics cannot include feedback processes such as Climate-Carbon Feedback (CCF). Therefore, there is a need to develop new emission metrics.

Neubauer and Megonigal (2015) presented two alternative metrics: the Sustained-Flux Global Warming Potential (SGWP) and the Sustained-Flux Global Cooling Potential (SGCP). Unlike traditional emission metrics, the SGWP includes feedback processes that account for gas fluxes that persist over time. The SGWP applies to gas emissions, which is similar to the traditional GWP, whereas the SGCP is a metric that applies to gas uptake and indicates how efficiently Earth processes reduce radiative forcing.

The SGWP and SGCP metrics have been widely used in representations of the impact of climate forcers in ecosystem studies. However, these two metrics provide only limited information compared to dynamic modeling. Therefore, new metrics are still required to simplify the measurement of the response of the climate system to the emission of climate forcers.

# 8. The Evaluation of Climate Model



## 8.1. Introduction

Climate modeling is an important tool for producing climatological fields for scenarios. Model development is an ongoing process, and the performance of models is being improved by the use of better spatial resolution and by including interactions between the Earth’s “spheres” (e.g., the atmosphere, ocean, cryosphere, aerosol, and biosphere). In this chapter, the appropriateness of using climate models to predict and analyze the future climate is described by presenting reviews on studies dating from 2014 onwards.

## 8.2. Global climate model

Global climate models generally reproduce historical climate conditions well although some biases still exist (solid agreement).

Global climate models covers the entire globe, which has zonally periodic space. This means that global models can predict the future because information around the target grid point is required to make predictions for that point. When a model calculates the future dynamical state from primitive equations, physical forcings such as radiation and land-surface processes are also considered. Following the publication of the IPCC’s Fifth Assessment Report in 2014, the Coupled Model Intercomparison Project phase 3 (CMIP3) and CMIP5 results have been widely

used in studies of the future climate. Recently, the CMIP6 results have been released and been used in several studies. The CMIP5 has an enhanced spatial resolution and includes the concept of Earth-system modeling. The CMIP3 system considers interactions between the ocean, cryosphere, and atmosphere. CMIP5 considers the additional effects of interactions with aerosols, chemical processes, land carbon, and ocean biogeochemistry on the CMIP3 system. One major difference between CMIP3 and CMIP5 is the way in which the effect of forcings on future climate change is represented. CMIP3 is based on the special report on emission scenarios (SRES), which is concerned with change scenarios for anthropogenic greenhouse gas concentrations. CMIP5 uses the representative concentration pathway (RCP) scenarios as the radiative forcing. The RCP scenario indicates that a single representative radiative forcing can result

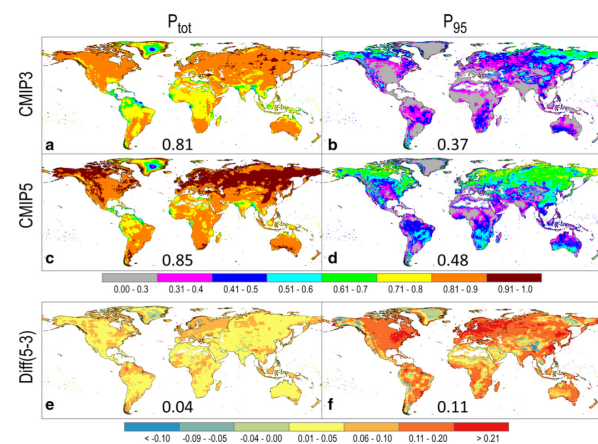


**Fig. 8.1.** PDF skill score of the total distribution of wet day precipitation ( $P_{tot}$ ) and higher percentiles ( $P_{95}$ ) from CMIP3 and CMIP5. (Koutroulis et al., 2016).

from several possible scenarios. CMIP6 is based on shared socio-economic pathways (SSPs) that take into account socio-economic factors. However, as CMIP6 has only just been released, there have been few studies on the East Asian monsoon system based on the CMIP6 results. Therefore, reviews of studies using CMIP6 are not included in this report.

Figure 8.1 shows the probability density function (PDF) skill score of precipitation ensemble results from CMIP3 and CMIP5. The overall skill score for CMIP5 is higher than that for CMIP3. Both CMIP3 and CMIP5 simulations perform better in middle and high latitude regions of the northern hemisphere—the score for these regions is high at 0.9. The performance of the simulations of intense precipitation is presented as 95<sup>th</sup> percentile scores, which show the improved ability of CMIP5 to simulate heavy precipitation. Also, CMIP5 shows improvements in terms of near-surface air temperature and long-term variability of sea surface temperature when compared to CMIP3. Studies on the east Asian monsoon system show that CMIP5 is better able to simulate the monsoon than CMIP3. However, despite these improvements, CMIP5 could not capture detailed features of the monsoon such as the meridional displacement of the Changma.

### 8.3. Regional climate model downscaling

Regional climate models with downscaled resolutions can simulate regional-scale phenomena over east Asia well (solid agreement).

Global climate models have limited ability to simulate detailed small-scale features due to their relatively lower resolution. To overcome this limitation, regional climate models with higher resolutions are used to identify detailed, regional-scale climate change. The COordinated Regional climate Downscaling Experiment (CORDEX) project is being operated under the World Climate Research Program (WRCP) in order to compare simulated results from multiple regional climate models over the same coordinated domains. The CORDEX project collects regional downscaled climate-change information from 14 different domains. Products from multiple regional models are used in ensembles to conduct high-confidence regional climate change information. The CORDEX-East Asia (EA) project performs regional

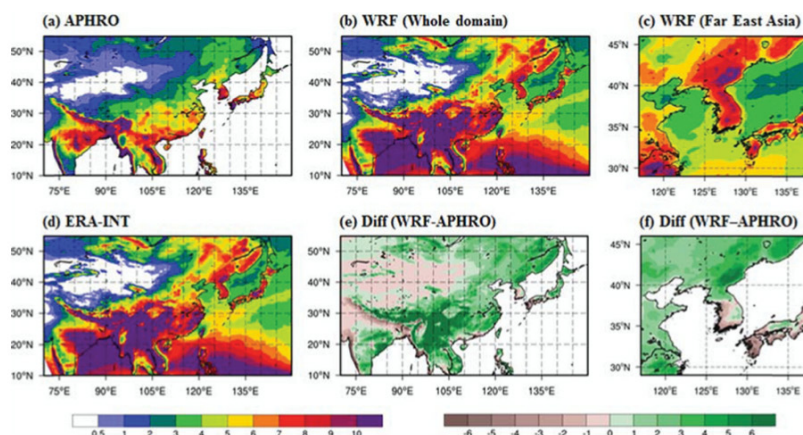


Fig. 8.2. Boreal summer precipitation climatology ( $\text{mm d}^{-1}$ ) with respect to (a) AHPRODITE, (b) WRF (Whole domain), (c) WRF (Far East Asia), (d) ERA-INT and bias of (e) WRF (Whole domain), (f) WRF (Far East Asia) compared with AHPRODITE (Ahn et al., 2018).

downscaling by using the CMIP5 results as the initial and lateral boundary conditions to work out the detailed effects of climate change on the east Asian monsoon system.

Ahn et al. (2018) analyzed downscaled historical results from the Weather Research and Forecasting (WRF) model from phase 2 of CORDEX-EA. The spatial distributions of summer and winter were evaluated with respect to observations (Fig. 8.2). The WRF model overestimated summer precipitation over the south Asia region, including the Indochina peninsula, whereas it underestimated summer precipitation over the Korean peninsula and the southern part of Japan. However, the downscaled results still generally agreed well with the observations.

The high-resolution configurations of regional climate models are able to reproduce mesoscale features such as typhoons. Multiple regional models that were part of CORDEX-EA simulated the distribution and numbers of typhoons well even though there was quite a large spread among the model results.

## 8.4. Regional coupled model

At the regional scale, atmosphere-ocean coupling can allow regional climate models to produce improved predictions over East Asia (solid agreement).

Recent research suggests that regional atmosphere-ocean coupling has significant effects over the east Asian region. In many studies it has been shown that air-sea interactions play an important role in the precipitation systems and large-scale circulation of the Asian monsoon, and so including this coupling in modeling can lead to improved predictions.

Ham et al. (2016) evaluated 25 years of historical simulations of the east Asian region by regional atmospheric models and coupled model systems. Global coupled model systems can improve the modeling of atmospheric heat fluxes and tropical Pacific precipitation bands; however, the coupling system induces errors in sea surface temperature

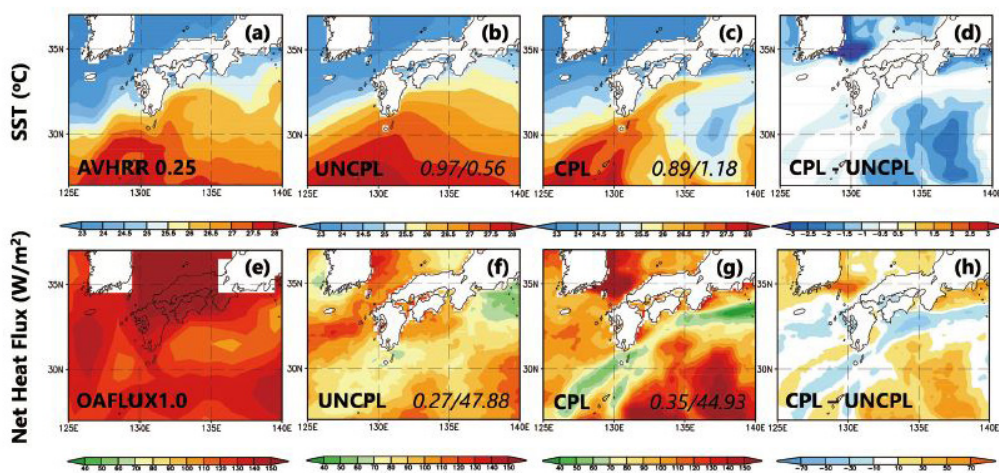
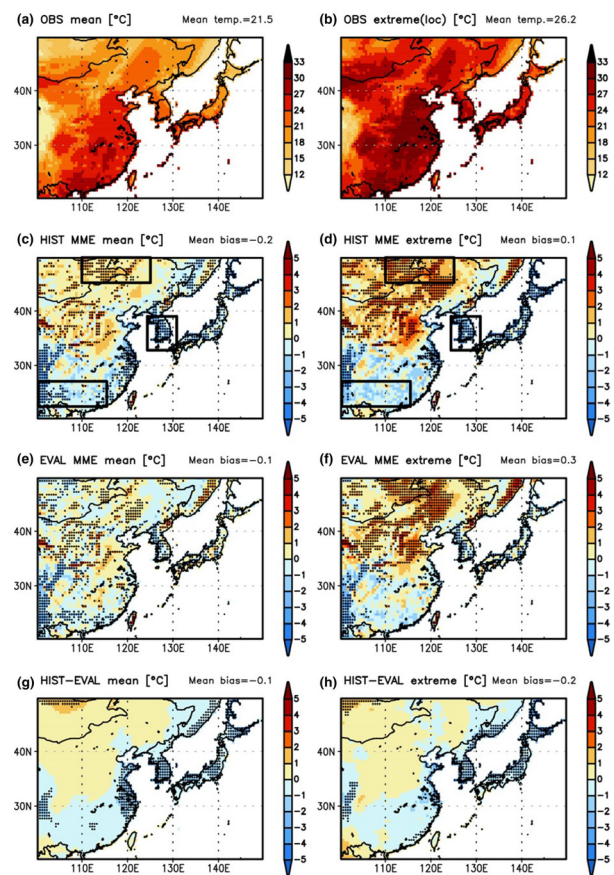


Fig. 8.3. Monthly averaged SST, net flux, and model difference for atmospheric model (UNCPL) and coupled model (CPL) in July 1987. (Ham et al. 2016).

(SST) modeling. Regional coupled models do not produce noteworthy improvements to the global coupled model. However, high-resolution regional coupling can improve the modeling of SST and net fluxes by enhancing the modeling of ocean current circulation in coastal regions (Fig. 8.3). As a result of these improvements and by considering interactions between the SSTs, radiative fluxes, and precipitation, realistic modeling of the atmospheric circulation can be produced. It should be pointed out that cloud-radiation interactions should also be taken into account in order to reduce SST biases.

## 8.5. Simulation of extreme events

It is important to present the possibility of extreme events in future climate change as well as the mean changes. Park et al. (2016) evaluated the performance of historical simulations of extreme events based on the results of five regional models that participated in CORDEX-EA. It was clearly shown that the high-resolution models could produce extreme events in the climate simulations. From these analyses, it is also clear that using the same regional model with different global forcing data produces similar biases relative to the observations. This means that the regional models have a much stronger impact on smaller-scale features in downscaled results than in the large-scale forcing. These results also suggest that multiple regional models are needed to assess regional future climate change properly.



**Fig. 8.4.** Spatial distributions of observed climatology (a, b), of RCM MME biases from the HIST (c, d) and EVAL (e, f) experiments, and of the differences (HIST minus EVAL; g, h) for JJA means (left) and extremes (right) of TAS (°C). Area mean values are given at the top right of each panel. (Park et al., 2016).

# 9. Detection of Climate Change and Changes in Meteorological Disasters on the Korean Peninsula



## 9.1. Introduction

In this section, the long-term trends and changes in climate phenomena in east Asia, including the Korean Peninsula, are analyzed and the causes of these changes and trends are evaluated. First, statistical detection studies of observed changes in temperature and precipitation over east Asia and studies of the attribution of changes to anthropogenic effects are assessed. Next, the latest research results on the observed changes in climate variability are summarized. This includes research on El-Niño, the Asian Monsoon, Arctic climate variability, and tropical intra-seasonal variability related closely to the Korean climate, as well to changes in meteorological disasters affecting the Korean Peninsula such as heatwaves, droughts, cold waves, heavy rainfall, and typhoons.

## 9.2. Temperature and precipitation changes in East Asia and the Korean Peninsula

The index of extreme warm extreme in summer has been increasing (solid agreement) and extreme precipitation events have been tending to increase in some regions (limited agreement).

The intensity, frequency, and duration of high-

temperature events have increased and low temperature-related indices have decreased across Asia since the 1950s, and this has been attributed to the increase in anthropogenic greenhouse gases. The probability of the occurrence of extreme summer heat events recently observed in east Asia was found to have been increased by anthropogenic forcing. Although there has been an increasing trend in extreme precipitation—for example, the maximum daily precipitation has increased in some regions—it is difficult to evaluate the effects of anthropogenic forcing due to the large influences of natural variables such as the El-Niño Southern Oscillation (ENSO).

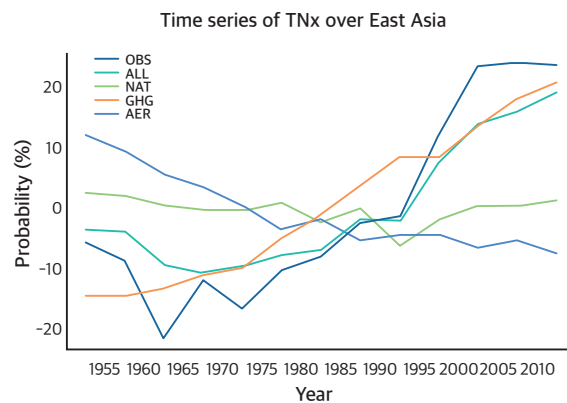


Fig. 9.1.1. 5-year mean time series of the annual maximum of the daily minimum temperature (TNx) averaged over east Asia (100°E - 157°E, 20°N - 50°N) for 1951~2015 based on HadEX3 observations (OBS, black), CMIP6 simulations with all forcing (ALL, green), natural forcing (NAT, blue), greenhouse gas forcings (GHG, red), and aerosol forcings (AER, purple)(Kim et al., 2016).

### 9.3. Changes in climate variability and their impacts on the Korean Peninsula

The impact of El-Niño on the climate in Korea is still unclear (limited agreement). Recently, precipitation related to the summer monsoon has been tending to decrease (intermediate agreement). The enhanced winter monsoon is contributing to the occurrence of cold waves

(limited agreement). Winter temperatures have been rising again recently in association with the Arctic Oscillation (solid agreement). The effects of sub-seasonal variability are present, but the cause of this variability is not yet clear (limited agreement).

El-Niño's impact on the Korean Peninsula's climate depends on the season and on the phase of El Niño. New studies have suggested precipitation and sea surface temperature variability in the western Pacific

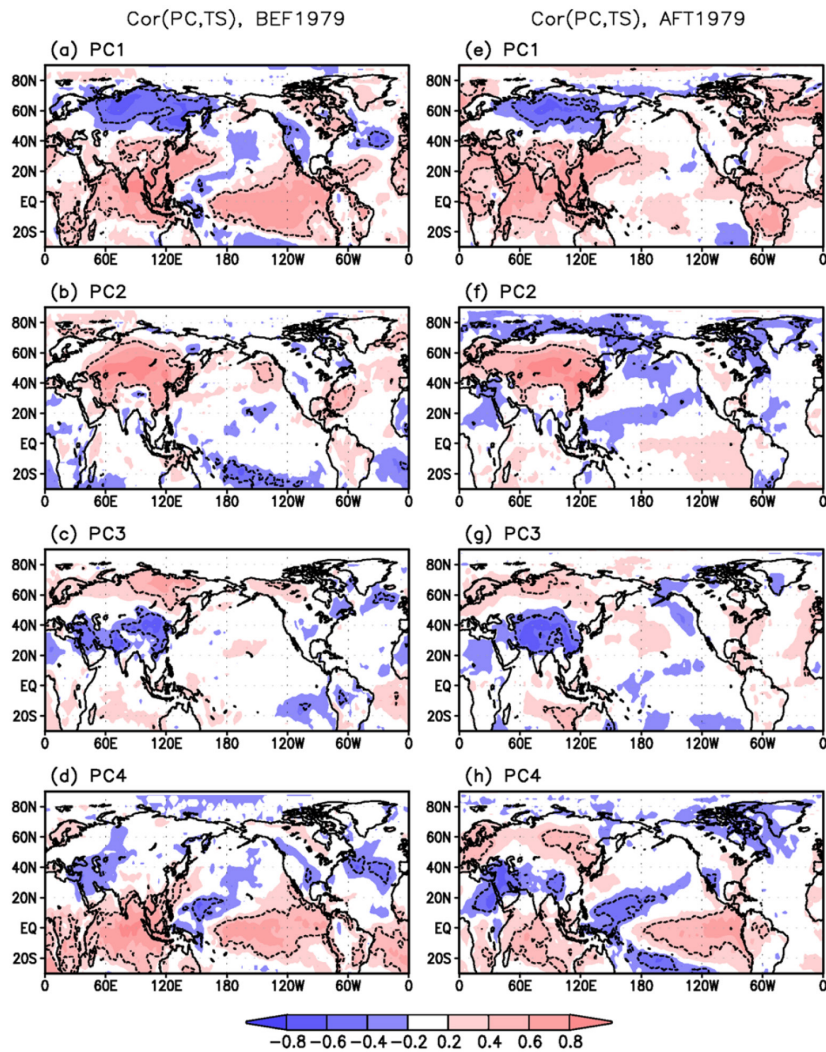
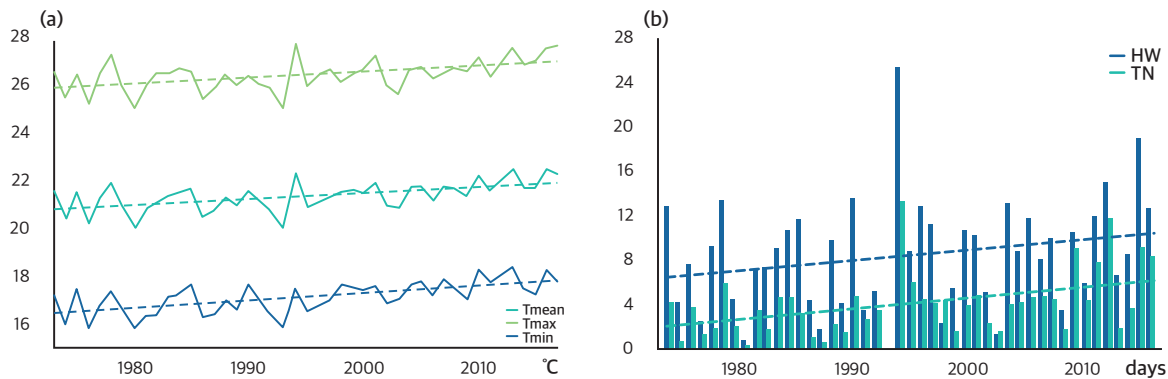


Fig. 9.2. The correlation between four major variability modes of the east Asian winter monsoon and sea surface temperatures. The dashed lines indicate statistical significance at the 95% confidence level (Yun et al., 2014).



**Fig. 9.3. (a) Time series of daily mean (black), maximum (red), and minimum (blue) temperatures from May to September for 1973~2017. (b) Bar graphs for occurrences of heat waves (red) and tropical nights (blue) (Choi and Lee, 2019).**

and subtropical oceans as a key causative process linked to the East Asian climate. How the variations in El-Niño affect the global and Korean climate remains unclear. Some impacts of the variations in the Indian Ocean and Atlantic Ocean on the Korean climate have, however, been identified.

In addition to the existing known causes, it has been newly identified that the east Asian summer monsoon is influenced by the interannual variability associated with tropical Atlantic sea surface temperatures, the Asian continental low- and upper-level jet streams, and the south Asian monsoon, as well as by various multi-decadal variations that occur over the North Atlantic and the tropical Indo-Pacific regions. In line with the long-term variability of the east Asian summer monsoon, the summer precipitation in Korea increased steadily from 1970 to the early 2010s, mainly during July and August, but has tended to decrease recently.

The variability in the east Asian winter monsoon can be generally divided into a northern mode, which is largely related to the intrusion of cold air masses from Siberia and to the Arctic Oscillation, and a southern mode, which is characterized by the ENSO-related variability of the east Asian trough and the Mongolian

High. These main modes exhibit long-term multi-decadal variability due to the effects of the Siberian High, the North Pacific Oscillation, and the Pacific Decadal Oscillation. The east Asian winter monsoon weakened from the mid-1970s to the mid-2000s and then intensified again afterwards. It has been suggested that the recent intensification of the east Asian winter monsoon is contributing to the increased occurrence of Korean cold waves.

The Arctic Oscillation Index steadily declined from the late 1990s to the 2000s, and has shown no significant change during the last decade. The Warm Arctic Cold Eurasia (WACE) mode associated with Arctic sea ice is not showing any prominent trend despite the recent decline in Arctic sea ice. As a result, the winter temperature over Korea decreased between 1990 and the early 2010s; it has recently increased again and is, therefore, changing in a non-linear way.

The amplitudes of the 10~20 day and 30~60 day sub-seasonal variability in summer have gradually increased in east Asia during the last 50 years. In particular, a strong intensification of the 10~20 day variability has been observed. The cause of this is, however, unclear and further research is needed.

## 9.4. Changes in meteorological disasters on the Korean Peninsula

The occurrence of tropical nights is clearly increasing (solid agreement). Winter and spring droughts are becoming worse (limited agreement), and heavy rainfall events are also increasing (intermediate agreement). Typhoon activity around the Korean peninsula is increasing in both frequency and intensity (intermediate agreement).

The frequency, intensity, and persistence of heat waves on the Korean Peninsula have increased since the 1970s, and the frequency of tropical nights has increased. The anthropogenic effects of increased greenhouse gases have been detected in recent cases of intense heatwave events affecting the Korean Peninsula. Heatwaves on the Korean Peninsula have been found to be affected by large-scale atmospheric circulations and various teleconnection patterns in addition to local and synoptic processes.

Annual precipitation in the Korean Peninsula has increased in recent decades, but with considerable seasonality. As a result, the frequency of droughts has decreased in summer, whereas it has increased in winter and spring.

The frequency of cold days and cold waves on the Korean Peninsula increased between the late 1990s and late 2000s. However, the changes thereafter have not been clear, and it is necessary to identify the causes and understand the synoptic structure of Korean cold waves.

The frequency and intensity of heavy rainfall events on the Korean Peninsula has tended to increase since the mid-1990s. This has been attributed to changes in teleconnections related to the tropics, changes in synoptic patterns around the Korean Peninsula, and increased typhoon activity.

Typhoon activity in the northwest Pacific has been declining recently, and it has been discovered that this decline is associated with changes in the sea surface temperature in the Northwest Pacific, the movement of tropical upper-air troughs, and increases in the sea surface temperature in the North Atlantic. Typhoon activity around the Korean peninsula has increased in frequency and intensity since the mid-1990s, and this has been linked to a weakening of vertical wind shear around the Korean Peninsula, westward movement of the subtropical northwest Pacific High, and rising sea surface temperatures around the Korean Peninsula.

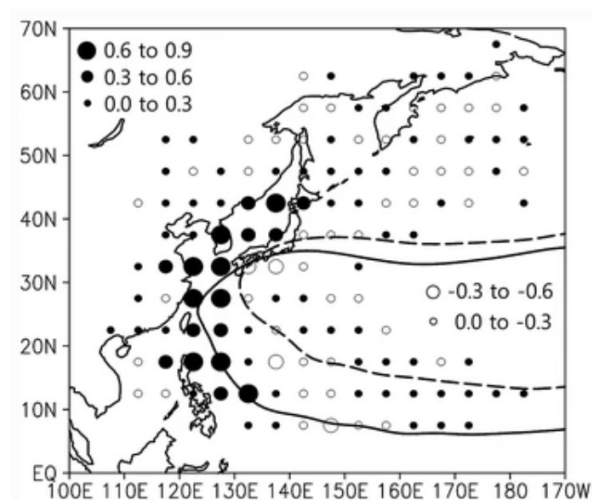


**Fig. 9.4.** Changes in typhoon track density between two periods (P1: 1965~1983, P2: 1984~2004). The dotted and solid lines represent the 5860gpm contours for P1 and P2 periods, respectively (Choi et al., 2017).

# 10. Short-term and Long-term Projections of Climate Change



## 10.1. Introduction

This section describes short-term (before 2050) and long-term (after 2050) future climate change on the Korean Peninsula in terms of the atmosphere, ocean and cryosphere, based on the results of the GCM (General Circulation Model) and the RCM (regional climate model), which featured in the IPCC Fifth Assessment Report. In addition, the prospects for climate stabilization based on strengthening pan-global action to limit global warming to 1.5°C are evaluated.

than 4°C following RCP 8.5 by the end of the 21<sup>st</sup> century (solid agreement). Precipitation is projected to increase based on both RCP 4.5 and RCP 8.5 by the end of the 21<sup>st</sup> century, but there is a difference in the trends between the models (intermediate agreement).

In the short-term outlook (202~2050) for temperature, precipitation, and extreme climate events, it is predicted that the average temperature will increase by 1.33°C to +1.93°C in all scenarios. The prediction based on the RCMs is for an increase in the range of +1.05°C to +1.95°C compared to the 1981~2005 average. The five RCMs show different patterns of warming in the short-term, but the results of these different model scenarios give temperature increases of 1.54°C, 1.68°C, 1.17°C, and 1.75°C for RCP 2.6 (Representative Concentration Pathway 2.6), RCP 4.5, RCP 6.0, and RCP 8.5, respectively. Meanwhile, short-term projections for annual precipitation on the

## 10.2. Atmosphere and indicators

In the future, the average annual temperature on the Korean Peninsula is expected to rise by more than 2°C following RCP 4.5 and by more

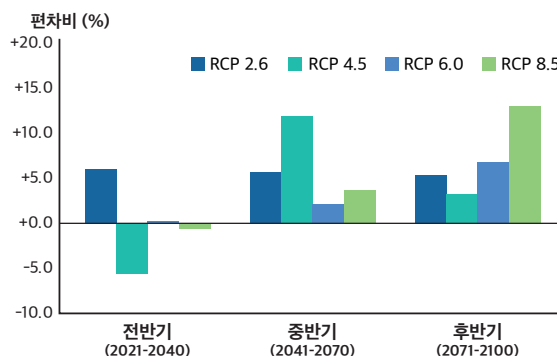


Fig. 10.1. Projections of annual precipitation deviation in the early, middle, and late 21<sup>st</sup> century compared to the 1981~2010 modeled climate (%) for four RCP scenarios (KMA, 2018)

Korean peninsula based on the RCMs vary more depending on the model, forecasting a 6.0% increase, 5.6% decrease, 0.2% increase, and 0.7% decrease for RCP 2.6, RCP 4.5, RCP 6.0, and RCP8.5, respectively. (Figure 10.1). Indices of extreme high temperatures such as the number of heatwave days, tropical nights, and summer days are expected to increase, while low temperature-related indices such as the number of cold wave days, ice days, and frost days are predicted to decrease. Extreme precipitation phenomena such as droughts and heavy rains are expected to become more frequent due to increased variability in precipitation.

In the long-term outlook (post-2050), the temperature for the period 2071~2100 is expected to be about 2.9

°C higher compared to the current climate according to RCP 4.5 and about 4.7°C higher according to RCP 8.5 (Figure 10.2). The increase in winter is expected to be higher than in summer.

For precipitation, the long-term forecast is more uncertain than for the temperature, with large differences between the models. According to the results of the CMIP5 climate models, the increase based on the RCP 8.5 scenario is greater (18%); however, according to RCP 4.5, precipitation is still forecast to increase by 16% by the second half of the 21<sup>st</sup> century. According to the RCM based on the RCP 8.5 scenario, the annual, summer, and winter precipitation on the Korean Peninsula is projected to increase by 19.1%,

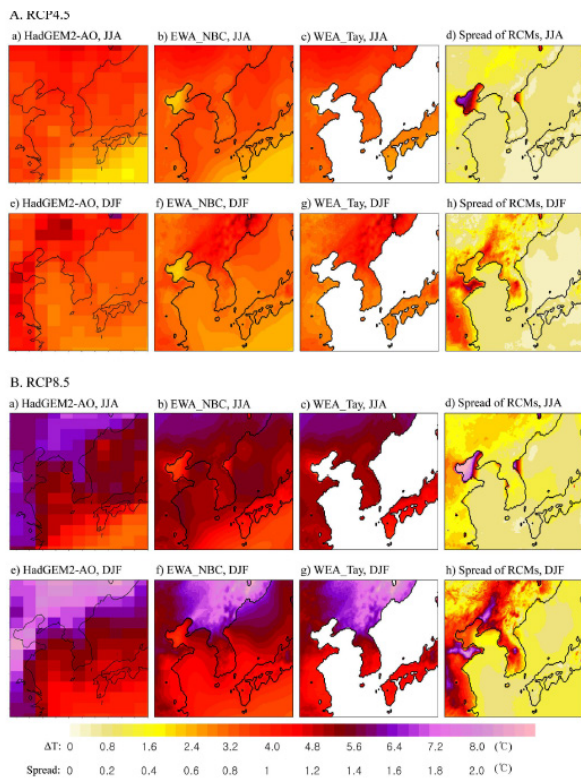


Fig. 10.2. Spatial distribution of projected summer (JJA) and winter (DJF) mean temperatures (°C) for the late 21<sup>st</sup> century (2076~2100) compared to the modeled current (1981~2005) climate based on the RCP 4.5 and RCP 8.5 scenarios. All changes are significant at the t-test 1% significance level (Suh et al., 2016).

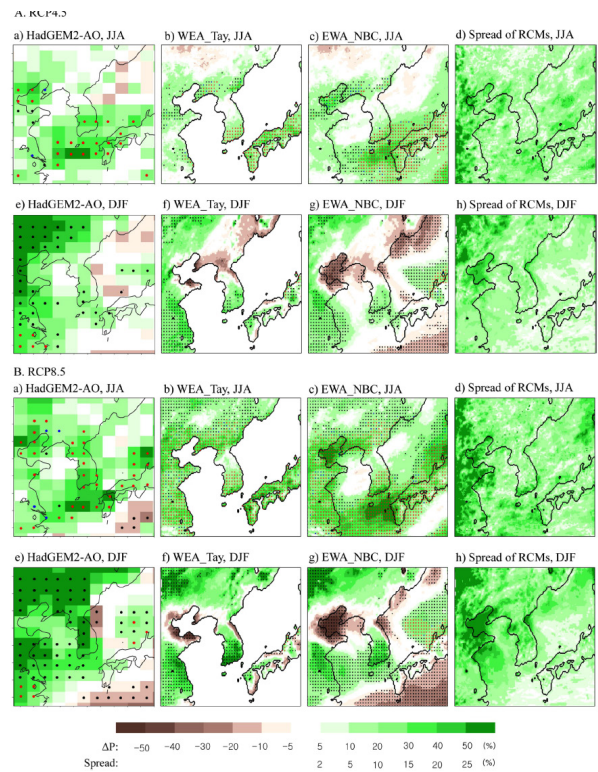
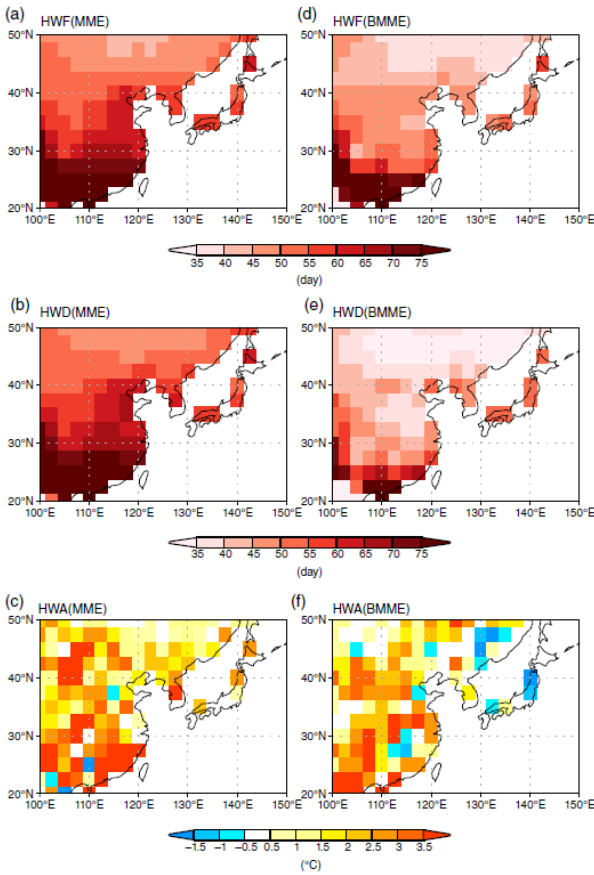


Fig. 10.3. Spatial distribution of projected summer (JJA) and winter (DJF) mean precipitation changes (%) during the late 21<sup>st</sup> century (2076~2100) compared to the modeled present (1981~2005) climate based on the RCP 4.5 and RCP 8.5 scenarios. The regions with black, blue, and red dots indicate precipitation changes with 10%, 5%, and 1% t-test significance levels, respectively (Oh et al., 2016).



**Fig. 10.4.** Projected changes in heatwave indices for 2075~2099: (a) HWF (yearly sum of heatwave days), (b) HWD (length of the longest yearly event), and (c) HWA (hottest day of hottest yearly event) for MME. (d)-(f) Same as (a)-(c) but for BMME (Seo et al., 2018).

20.5%, and 33.3%, respectively by the second half of the 21<sup>st</sup> century (Figure 10.3).

Both the intensity and frequency of heatwaves are projected to increase by the end of the 21<sup>st</sup> century. In particular, five CMIP5 models with relatively good simulation abilities project that, based on RCP 4.5, by the late 21<sup>st</sup> century the heatwave frequency index will increase by 52.5 days, the heatwave duration index will increase by 44.5 days, and the heatwave temperature index will rise by 2.2°C compared to current conditions (figure 10.4).

Increases in precipitation are projected in both the RCP 4.5 and RCP 8.5 scenarios, not only in terms of mean precipitation but also in terms of extreme

precipitation and frequency. The likely maximum precipitation will also increase by the end of the 21<sup>st</sup> century.

### 10.3. The ocean and the cryosphere

The water temperature in the East Sea is expected to increase continuously due to global warming, and this is believed to be caused by an increase in heat transport to the East Sea via the Tsushima currents. The temperature of cold water near the sea floor in the Yellow Sea, which has a significant impact on the Yellow Sea ecosystem, is expected to gradually increase by 2100 (solid agreement). By 2100, the mean sea level around the Korean Peninsula is projected to increase by 37.8 cm in RCP 2.6, 37.8 cm in RCP 4.5, 48.1 cm in RCP 6.0, and 65.0 cm in RCP 8.5, which is slightly less than the global average (solid agreement). It has been reported that, according to models that take account of the melting of Antarctic ice, the increase may be more than 130 cm, depending on the scenario (limited agreement). The rapid decline in the area and thickness of Arctic sea ice will continue throughout the early part of the 21<sup>st</sup> century. Autumn sea ice is expected to disappear by 2050 (intermediate agreement).

The sea surface temperature in the East Sea is expected to increase due to the increased heat transport by the Tsushima current. It is also expected that the temperature of the cold water near the floor of the Yellow Sea, which has a significant effect on the Yellow Sea ecosystem, will gradually increase by 2100.

It is expected that the East Sea Ocean temperature will rise as the amount of water entering the East Sea

increases and the ocean temperature increases. These projections are based on the results produced by the CMIP5 models.

Also, it is expected that the surface water temperature will rise by more if the East Korea Warm Current reaches higher-latitude waters. The East Korea Warm Current is an important factor to consider when studying future trends in the temperature of the East Sea. The sea level around the Korean peninsula has risen by about 10 cm in the last 40 years. In Korea, in the 29 years from 1989 to 2017, there was an annual rate of increase of 2.9 mm, which is rather rapid compared to the global average. Regionally, Jeju had the greatest rise (4.44 mm), followed by the east coast (3.70 mm), south coast (2.41 mm), and west coast (2.07 mm).

By the end of the 21<sup>st</sup> century, Korea's average sea level is projected to rise by 37.8 cm, 48.1 cm, 47.7 cm, or 65.0 cm based on RCP 2.6, RCP 4.5, RCP 6.0, and RCP 8.5, respectively. These rises are in proportion to the increase in greenhouse gas emissions and are lower than the global average in RCP 8.5. In terms of the regional differences in sea level, the sea level rise is expected to be higher in the South Sea region than in other regions and slightly lower in the west coast region than in other regions.

If current trends in greenhouse gas emissions continue, based on modeling that takes into account Antarctic ice sheet melting, average global sea level rise is predicted to reach 130 cm by 2100. In Korea, if the sea level in the coastal region rises by 1 m, 1.2% of the Korean peninsula's area is expected to flood.

Observations have shown that the Arctic sea ice area in September is linearly related to cumulative CO<sub>2</sub> emissions. The sea ice area is decreasing by  $3 \pm 0.3 \text{ m}^2$  per ton of CO<sub>2</sub> emissions. Based on this relationship, it can be estimated that by the time an additional 1000 Gt of CO<sub>2</sub> has been released, the Arctic sea ice in September will almost have disappeared. This means that if the current annual

rate of 35 Gt of emissions is maintained, the ice is expected to disappear before the middle of the 21<sup>st</sup> century.

#### 10.4. 1.5°C Climate change projection

Along with future (2091~2100) global warming of 1.5°C, the temperature change in east Asia and the Korean peninsula is expected to be consistent with global projections. The change in precipitation is expected to be slightly greater than the global change (solid agreement).

Applying five different climate models to a historical 10-year period (2006~2015) and 1.5°C future warming scenarios (2091~2100), the monthly-mean temperature in the Korean Peninsula is projected to increase by 0.8°C while the maximum and minimum monthly temperature would increase by 0.89°C and 0.91°C, respectively. Precipitation is expected to increase by 62.26 mm.

Extreme temperatures and precipitation are tending to lead to a wider probability distribution function as the standard deviation increases, and the frequency of extreme high temperatures and precipitation amounts above the 90<sup>th</sup> percentile are expected to increase by about 10% compared to the present. The probability of low temperatures and precipitation amounts below the 10<sup>th</sup> percentile is expected to decrease. The probability distributions showed more obvious changes in terms of extreme monthly maximum and minimum values than in average monthly temperatures.

## Summary for Policymakers

# Korean Climate Change Assessment Report 2020 - The Physical Science Basis -

---

**Published by** Administrator, Korea Meteorological Administration  
**Edited by** KIM Nam Ouk, Lee Jeung Whan, Cho Kuh hee, Kim Sang hoon (KMA)  
**Publication Date** July, 2020

61, 16-Gil, YeoUiDaeBang-Ro, Dongjak-Gu, Seoul, Republic of Korea (ZipCode 07062)  
T. +82-2-2181-0393, 0404 F. +82-2-2181-0469 W. <http://www.kma.go.kr>

---

ISBN 978-89-954715-9-3

Summary for Policymakers

# Korean Climate Change Assessment Report 2020

- The Physical Science Basis -



Korea Meteorological  
Administration

ISBN 978-89-954715-9-3